Geology, geochronology, and geochemistry of Isla María Madre, Nayarit, Mexico

Valerie Pompa-Mera[1,*], Peter Schaaf[2], Teodoro Hernández-Treviño[2], Bodo Weber[3], Gabriela Solís-Pichardo[4], Daniel Villanueva-Lascurain[1], and Paul Layer[5]

[1] Posgrado en Ciencias de la Tierra, Instituto de Geofísica, Universidad Nacional Autónoma de México, 04510 México, D.F., Mexico.
[2] Laboratorio Universitario de Geoquímica Isotópica (LUGIS), Instituto de Geofísica, Universidad Nacional Autónoma de México, 04510 México, D.F., Mexico.
[3] Departamento de Geología, CICESE, Carretera Ensenada-Tijuana 3918, 22860 Ensenada, B.C., Mexico.
[4] Laboratorio Universitario de Geoquímica Isotópica (LUGIS), Depto. de Geoquímica, Instituto de Geología, Universidad Nacional Autónoma de México, 04510 México, D.F., Mexico.
[5] Geophysical Institute and Department of Geology and Geophysics, University of Alaska Fairbanks, Fairbanks, AK, U.S.A.
** valerie@geofisica.unam.mx*

ABSTRACT

Islas Marías archipelago is located 110 km NW of San Blas, Nayarit in the mouth of the Gulf of California. The archipelago is formed by San Juanito, María Madre, María Magdalena, and María Cleofas islands. The position of these islands represents a key point for paleogeographic and paleotectonic reconstructions of northwestern Mexico and of the tectonic evolution of Baja California Peninsula. María Madre is the largest island and covers an area of 145 km^2. This study presents the first detailed geological map of the island together with geochemical and geochronological data of its lithological units.

Isolated basement rocks are exposed along the western coast in the form of migmatites and orthogneisses of granodioritic to granitic compositions and middle Jurassic ages (163 – 170 Ma). In the west-central part, a metasedimentary sequence, with biotite ± garnet paragneisses and folded calcsilicate rocks with or without garnet bands of unknown ages, is exposed as a roof pendant of the underlying Cretaceous intrusions (80.8 – 83.4 Ma) of tonalitic to granitic compositions. These granitoids are cut by mafic and pegmatitic dikes. We named the overall assemblage of metamorphic and plutonic rocks as "Papelillo Complex" due to the predominant outcrops in the homonymous canyon. The Papelillo Complex is overlain by ignimbrites, volcanic breccias, and lava flows of rhyolitic compositions. $^{40}Ar/^{39}Ar$ geochronology in sanidines from these rocks yielded Cretaceous (71.6 – 80.6 Ma) and Tertiary (55.4 Ma) ages, suggesting contemporaneous volcanic and plutonic activity. This inference is confirmed by similar REE patterns in both units with typical distributions for a subduction-related magmatic arc environment.

Towards the east, the igneous sequence is covered by Late Miocene to Pleistocene? marine and shallow marine deposits and towards the south by an Early Miocene? clastic continental sequence (informally named Isla Magdalena sandstone). Marine and shallow marine sediments were informally named "Ojo de Buey sequence" and subdivided into a lower and an upper member. Detrital zircon ages from both units display major peaks at ca. 83 Ma, indicating sedimentation mainly from plutonic and volcanic rocks of the same age. In the Ojo de Buey sequence, no zircons younger than Late Cretaceous were found. The Isla Magdalena sandstone, instead, shows a prominent peak at ~22 Ma, suggesting detritus from a different igneous source.

The lithologies of Isla María Madre are similar to those from the Los Cabos Block in Baja California

Pompa-Mera, V., Schaaf, P., Hernández-Treviño, T., Weber, B., Solís-Pichardo, G., Villanueva-Lascurain, D., Layer, P., 2013, Geology, geochronology, and geochemistry of Isla María Madre, Nayarit, Mexico: Revista Mexicana de Ciencias Geológicas, v. 30, núm. 1, p. 1-23.

Sur and from central Sinaloa. The overall area forms part of a Cretaceous plutonic belt, which definitely rules out large latitudinal displacements for the southern Baja California Peninsula.

Key words: geochemistry, geochronology, paleogeography, Isla María Madre, Gulf of California, Mexico.

RESUMEN

El archipiélago de las Islas Marías se ubica a 110 km al noroeste de San Blas, Nayarit, en la desembocadura del Golfo de California. El archipiélago está formado por las islas San Juanito, María Madre, María Magdalena y María Cleofas. La ubicación de estas islas representa un punto clave para las reconstrucciones paleogeográficas y paleotectónicas del noroeste de México y la evolución tectónica de la Península de Baja California. La Isla María Madre es la isla más grande y abarca una superficie de 145 km^2. Este estudio presenta el primer mapa geológico detallado de la isla, junto con datos geoquímicos y geocronológicos de sus unidades litológicas. Las rocas basales están expuestas a lo largo de la costa oeste y consisten en migmatitas y ortogneises de composición granodiorítica a granítica con edades del Jurásico Medio (163–170 Ma). En la parte centro-oeste, una secuencia metasedimentaria con paragneises de biotita ± granate y calco-silicatos deformados con o sin bandas de granate, de edades desconocidas, está expuesta como un colgante de los intrusivos cretácicos subyacientes (80.8–83.4 Ma) que son de composiciones tonalíticas a graníticas. Estos cuerpos están cortados por diques máficos y pegmatíticos. Al conjunto total de rocas metamórficas y plutónicas lo hemos nombrado "Complejo Papelillo" debido a sus afloramientos en el cañón homónimo. El Complejo Papelillo está sobreyacido por ignimbritas, brechas volcánicas y flujos de lava de composición riolítica. Geocronología con el método $^{40}Ar/^{39}Ar$ en sanidinos de éstas rocas reveló edades cretácicas (71.6–80.6 Ma) y terciarias (55.4 Ma), sugiriendo una actividad volcánica contemporánea con el ensamble plutónico. Esta inferencia se confirmó mediante patrones similares de elementos de las Tierras Raras en ambas unidades con distribuciones típicas para un ambiente de arco magmático relacionado a subducción. La secuencia ígnea está cubierta en la parte este de la isla por depósitos marinos del Mioceno tardío – Pleistoceno? y localmente hacia el sur por una secuencia continental de areniscas del Mioceno temprano, similar a la observada en la isla vecina María Magdalena (nombrada informalmente arenisca Isla Magdalena). Los sedimentos marinos fueron nombrados informalmente "secuencia Ojo de Buey", dividida en un miembro inferior y uno superior. Edades de zircones detríticos de ambas unidades muestran picos mayores a ca. 83 Ma, que concuerdan con las edades de rocas plutónicas y volcánicas. En la formación Ojo de Buey no se encontraron edades más jóvenes. Por otra parte, zircones de la formación Isla Magdalena muestran un pico prominente a ~22 Ma, sugiriendo detritos de una fuente ígnea distinta.

La litología de la Isla María Madre es muy similar a la del Bloque Los Cabos en Baja California Sur y a la de Sinaloa Central (Complejo Volcánico Inferior de la Sierra Madre Occidental). El área en su totalidad forma parte de un cinturón cretácico común, lo cual definitivamente excluye grandes desplazamientos latitudinales para el sur de la Península de Baja California.

Palabras clave: geoquímica, geocronología, paleogeografía, Isla María Madre, Golfo de California, México.

INTRODUCTION

Islas Marías archipelago is located in the mouth of the Gulf of California, 110 km NW of San Blas, in the state of Nayarit, Mexico, and 220–270 km southeast of Baja California Peninsula (Figure 1a). From northwest to southeast, the archipelago consists of four islands: San Juanito, María Madre, María Magdalena and María Cleofas (Figure 1b). In the literature, San Juanito island is often not considered part of the archipelago, which is consequently often named "Tres Marías Islands". María Madre (21°31'–21°40' N and 106°30'–106°38' W) is the largest island of the archipielago, covers an area of 145 km^2, and hosts the Islas Marías Federal Penal Colony. The Mexican Navy provides transportation facilities in a weekly connection between Mazatlán, Sinaloa, and Balleto (Figure 2). Climate is dry with moderate rainfall from June to October. The Islas Marías archipelago conserves important ecosystems, including some endemic fauna and flora species, and forms part of the "Protected Areas of the Gulf of California" by the Comisión Nacional de Areas Naturales Protegidas (CONANP) of the Mexican Ministry of Environment and Natural Resources.

Tectonically, the islands are placed in an intermediate position between the northwestern edge of the Middle America Trench and the southeastern limit of the Tamayo Fracture Zone of the Rivera Plate, with the Tres Marías Escarpment to the west and southwest (Figure 1a). This

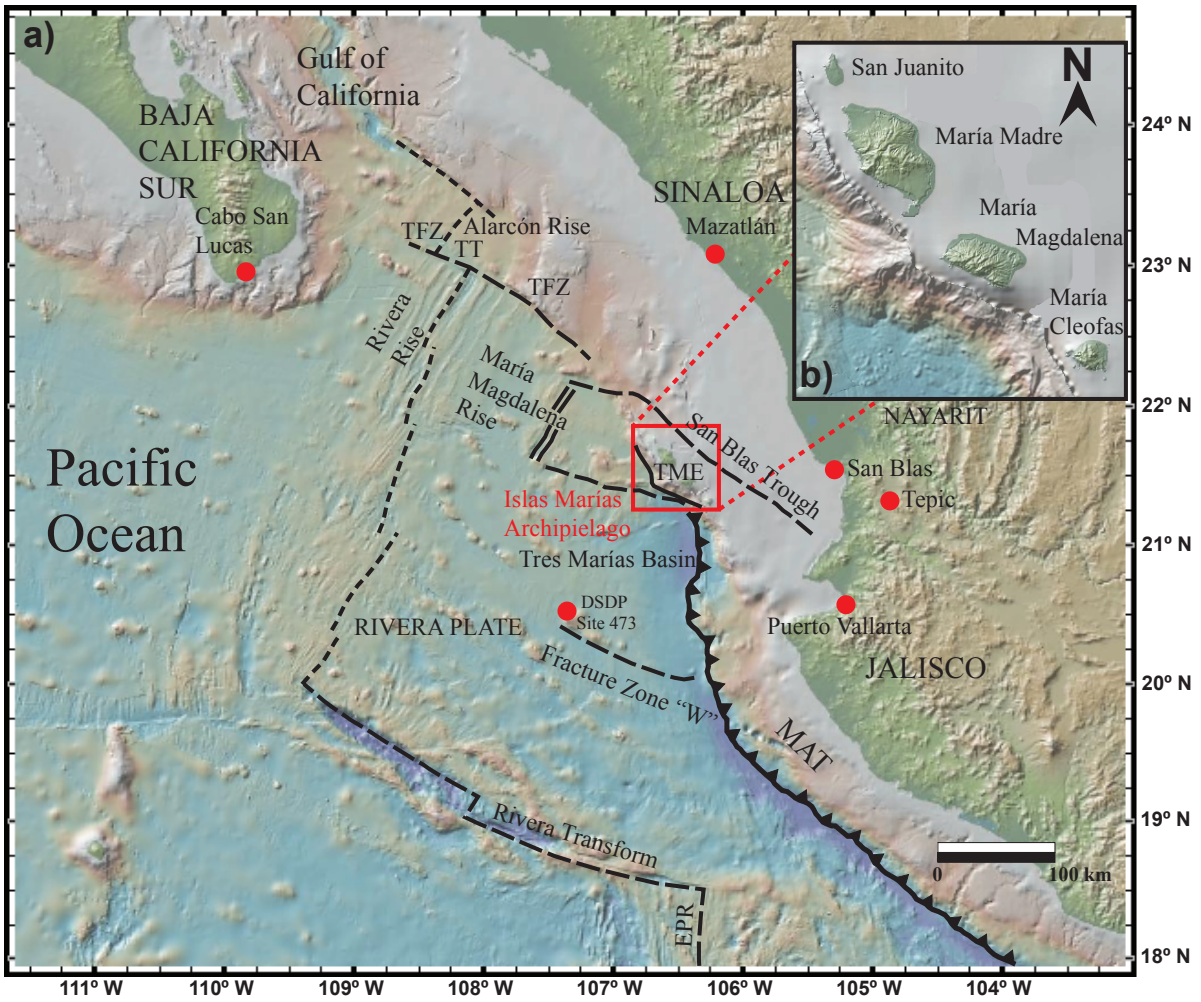

Figure 1. Global Multi-Resolution Topography (GMRT) synthesis map (modified from Ryan *et al.*, 2009) with tectonic features of the Pacific Ocean off northwestern Mexico. a) Location of the study area (red square). EPR = East Pacific Rise; MAT = Middle America Trench; TFZ = Tamayo Fracture Zone; TME = Tres Marías Escarpment; TT = Tamayo Transform. b) Inset with the four islands forming the Islas Marías Archipelago.

tectonic boundary between oceanic and continental lithosphere has a relief of more than 3000 m (Lonsdale, 1995). On the other hand, the ocean floor between the archipelago and mainland Mexico (Sinaloa and Nayarit) is a relatively shallow continental shelf with sedimentary basins (*e.g.*, San Blas Trough, Figure 1a).

The geology of Islas Marías constitutes a key point for paleogeographic reconstructions of the Baja California Peninsula. The study and correlation between rocks of Baja California and adjacent provinces of Cordilleran Mexico also contributes to the understanding of the tectonic processes involved in the opening of the Gulf of California since Late Miocene. During the last decades, investigations on granitic rocks of Sinaloa (Henry and Fredrikson, 1987), Nayarit and Jalisco (Schaaf *et al.*, 1995, 2000) as well as from the Los Cabos Block in Baja California Sur (Schaaf *et al.*, 2000) pointed to a common magmatic evolution. These plutonic rocks are regarded as a southward continuation of the Cordilleran Batholiths of California (*e.g.*, Peninsular Ranges) and Baja California (Henry *et al.*, 2003).

In this paper, updated information on the geological units of Isla María Madre is provided, accompanied by a new geological map and a stratigraphic column of the island. Besides that, the first geochemical analyses of the most representative rock units as well as the first U-Pb and $^{40}Ar/^{39}Ar$ geochronological data are presented. The results are integrated in a preliminary model for the geological evolution of the archipelago and its paleotectonic position with respect to mainland Mexico and Baja California.

PREVIOUS WORK

Studies on the Islas Marías geology are sparse. Early works in the area are mostly paleontological studies (Grayson, 1871; Nelson, 1899). In 1925, members of the California Academy of Sciences visited the Tres Marías Islands and reported Miocene diatomites from various expo-

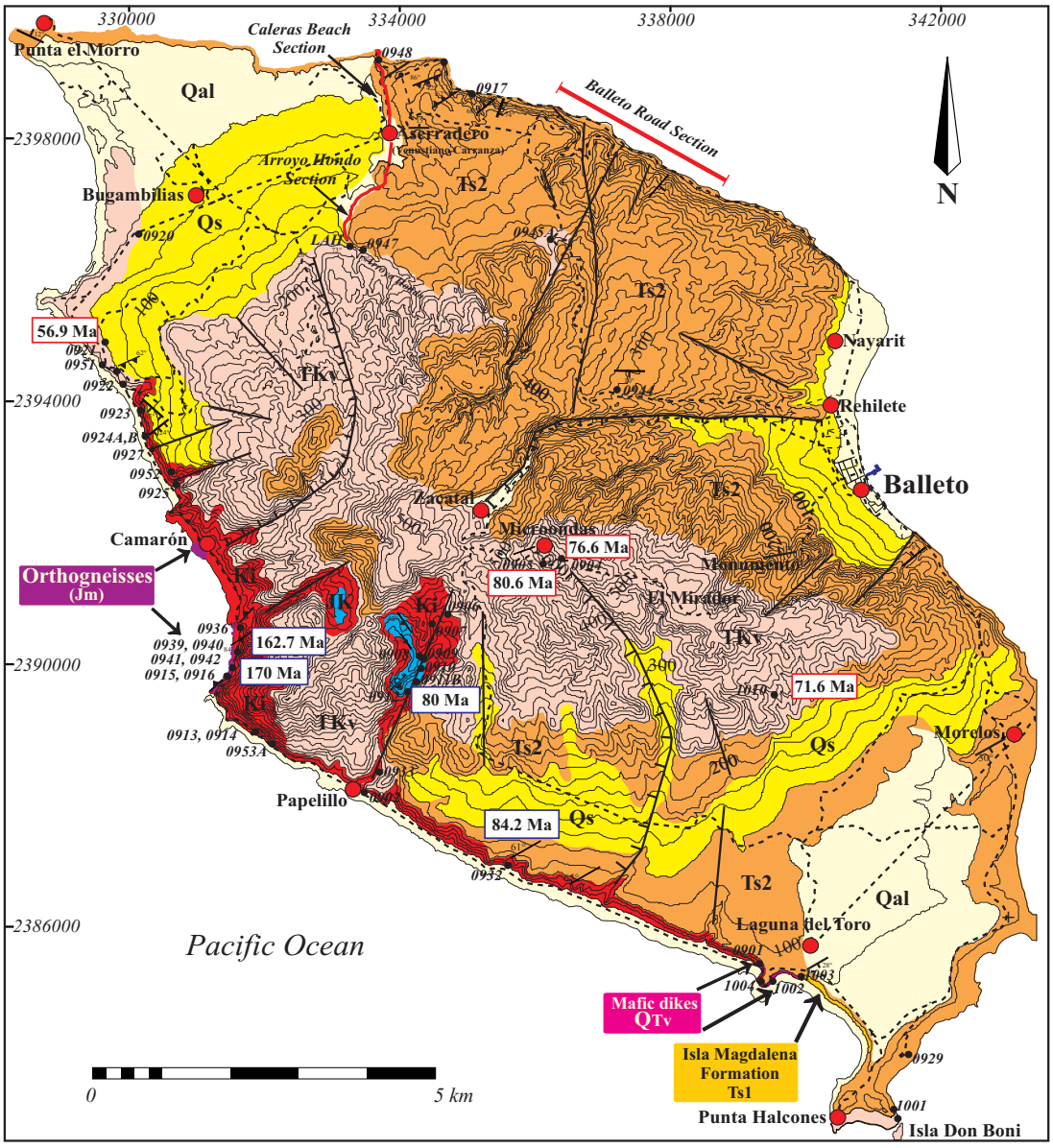

GEOLOGY OF ISLA MARÍA MADRE

Legend

- **Qal** Quaternary coastal and alluvial deposits
- **Qs** Quaternary colluvial deposits
- **QTv** Mafic dikes
- **Ts2** Tertiary sedimentary rocks (Ojo de Buey Formation)
- **Ts1** Tertiary sedimentary rocks (Isla Magdalena Formation)
- **TKv** Cretaceous-Tertiary volcanic rocks
- **Ki** Cretaceous plutonic rocks
- **JK** Jurassic-Cretaceous? Metasedimentary rocks
- **Jm** Jurassic banded and folded gneiss

Symbology

- Folding
- Reverse fault
- Normal fault
- Foliation
- Lineament
- Bedding
- Unpaved road
- Topographic point
- Sampling location
- Ar-Ar — Ar-Ar ages
- U-Pb — U-Pb ages
- Measured section by Carreño (1985) and McCloy *et al.* (1988)

Figure 2. Geological map of Isla María Madre with sampling locations and geochronological information.

sures as well as a brief description of the geology of María Madre and María Magdalena islands (Hanna and Grant, 1926; Jordan and Hertlein, 1926). Hertlein and Emerson (1959) performed a general description of macrofauna from material collected during the Puritan Expedition. Chiñas (1963) published the first geological description of outcrops from all four islands, along with a geological map of Isla María Madre, and a list of fossils in Miocene sediments. The author suggested that the islands formed as the result of Mesozoic to Tertiary tectonic processes and that the granitic rocks might be contemporaneous to those from Jalisco and Baja California. Brunner (1971) identified Miocene microfossils in diatomitic sequences, and Ramírez-Rubio (1980) aimed at possible petroleum resources in Tertiary sediments around the Tres Marías Islands. In the last decades, several micropaleontological studies (Carreño *et al.*, 1979; Carreño, 1985; Pérez-Guzmán, 1985; McCloy *et al.*, 1988) focused on biostratigraphy, age, and paleoenvironments of Neogene sedimentary sequences. Repeated subsidence and uplift events that are recorded in Late Miocene to Pleistocene sediments were related to the opening of the Gulf of California (McCloy *et al.*, 1988).

During the Deep Sea Drilling Project Leg 63 campaign, Site 473 was drilled approximately 90 km southwest of the Islas Marías Archipelago (Figure 1a). From this project resulted stratigraphical, bathymetrical, geochronological, and geochemical data for the ocean floor as well as evidence for the initial opening of the Gulf of California (*e.g.*, Bukry, 1978; Ness, 1982; Verma, 1983).

GEOLOGY OF ISLA MARÍA MADRE

In this work, geological reconnaissance studies and mapping were performed with emphasis on the coastal plains around the Isla María Madre. A moderate relief allows identifying major lithologies and contacts. North to south and east to west oriented roads and paths, like that from Papelillo to Microondas (Figure 2), show excellent rock exposures and were traversed by foot. Although moderate to thick vegetation covers many inland parts of the island, some contacts between major rock types can be located reasonably well on aerial photographs. During fieldwork, we verified and corrected a photogeological map previously prepared using 1:70 000 scale vertical air photos (INEGI, 1995). Subsequently, from our observations, and using the 1:50,000 scale topographical map (F13-C25; INEGI, 2000), a geological map was constructed (Figure 2).

A petrographic study of the different rock units was carried out in thin sections for rock classification and the results (Table 1) were also used to select samples for geochemical and geochronological investigations.

An outstanding morphological feature of Isla María Madre is a 600 m high, elongated mountain range in the central part, with the major axis oriented NW-SE. Steep slopes at the western part show excellent exposures of crystalline rocks. In the northern part, sedimentation and weathering processes have formed coastal deposits and terraces and, towards the east, colluvial and alluvial deposits control the morphology.

A remarkable attribute of María Madre Island is the lithological diversity found in an area of only 145 km^2. Metamorphic basement rocks (gneiss and metasediments), granitoids, volcanic units, and several types of sedimentary rocks are exposed (Figure 2).

Basement rocks

Outcrops of metamorphic basement rocks occur in a small segment along the western coast between Papelillo and Camarón (Figure 2) and are mainly formed by orthogneiss and paragneiss with different metamorphic textures.

Orthogneiss

Two orthogneiss types were distinguished in the field. The first one is represented by quartz-rich, folded, and banded migmatites (sample 0915, Figure 3a; sample 0939), which are coarse- to medium-grained, with 2 mm to ~5 cm thick leucocratic and mesocratic bands. The neosome is composed of quartz, potassium feldspar, plagioclase, biotite, garnet, and occasionally muscovite. The melanosome is formed by quartz, plagioclase, aligned biotite, and chlorite. Less abundant minerals are oxides, apatite, and zircon. A heterogranular mosaic with slightly strained biotite and quartz defines the texture of these rocks. Some parts of sample 0939 present millimeter- to centimeter-sized

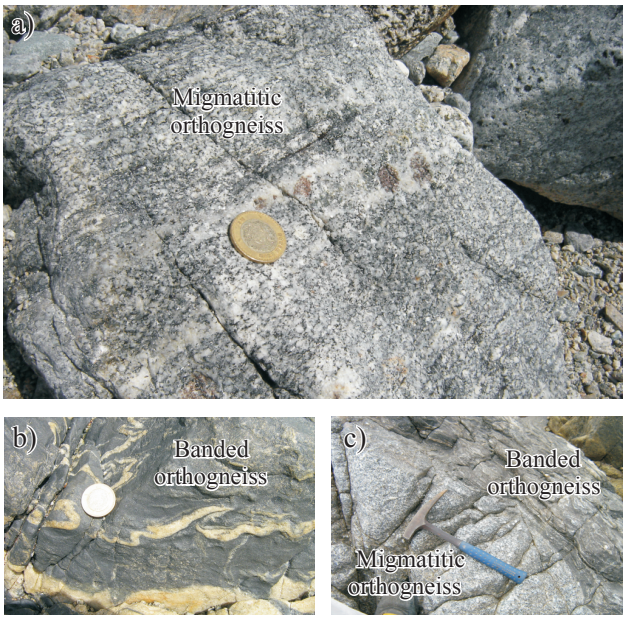

Figure 3. Metamorphic basement rocks of Isla María Madre. a) Migmatitic orthogneiss (sample 0915). b) Banded and foliated orthogneiss (samples 0939 and 0936). c) Banded orthogneiss in contact with the migmatitic orthogneiss (sample 0916).

garnet cumulates.

The second orthogneiss type shows dark grey colors (sample 0916), with banding, ptygmatic folding, and a granolepidoblastic texture (Figure 3b). The mineral paragenesis is quartz, potassium feldspar (microcline), plagioclase, biotite, muscovite, apatite, zircon, and opaque minerals as well as chlorite. This rock is observed in contact with the migmatites described above (Figure 3c).

Metasedimentary rocks

Outcrops of metasedimentary rocks, which are affected by contact metamorphism, are also restricted to the western sector of the island (Figure 2), three kilometers to the NE of Papelillo in the homonymous canyon. Four different units were identified:

1) At the slopes of the Papelillo canyon, biotite-garnet-bearing paragneisses are exposed (Figure 4a) in several locations (*e.g.*, sample 0909). The dark grey colored rocks have a massive and homogeneous appearance in the field. In thin section they display granolepidoblastic textures with quartz, abundant biotite, potassium feldspar, garnet, plagioclase, pyrite, and zircon. This unit is in contact with a tonalitic body (Figure 4a).

2) Intensely folded calcsilicates are composed of wollastonite, clinopyroxene, dolomite, quartz, and plagioclase (sample 0908; Figure 4b). The calcsilicate rocks together with the paragneisses mentioned above are suggestive of contact metamorphism.

3) Close to the contact with the younger plutonic rocks, outcrops of calcsilicates with a granoblastic mosaic of fine-grained wollastonite, dolomite and quartz bands were observed (Figure 4c).

4) The immediate contact of the calcsilicates with the intrusive rocks is characterized by occurrences of exo-skarn, composed of garnet, clinopyroxene (diopside), wollastonite, and quartz (sample 0910; Figure 4d). The skarn is reddish and has a granoblastic texture with monomineralic zones of garnet and wollastonite. Clinopyroxene is observed as inclusions in garnet bands or as glomerocrystals in wollastonite bands.

The metasedimentary assemblage of the Papelillo canyon is interpreted as a roof pendant in the granitoid rocks described in the following section.

Intrusive rocks

Outcrops of intrusive rocks are widely distributed along the western coast and in the slopes of Isla María Madre (Figure 2), and they probably underlie

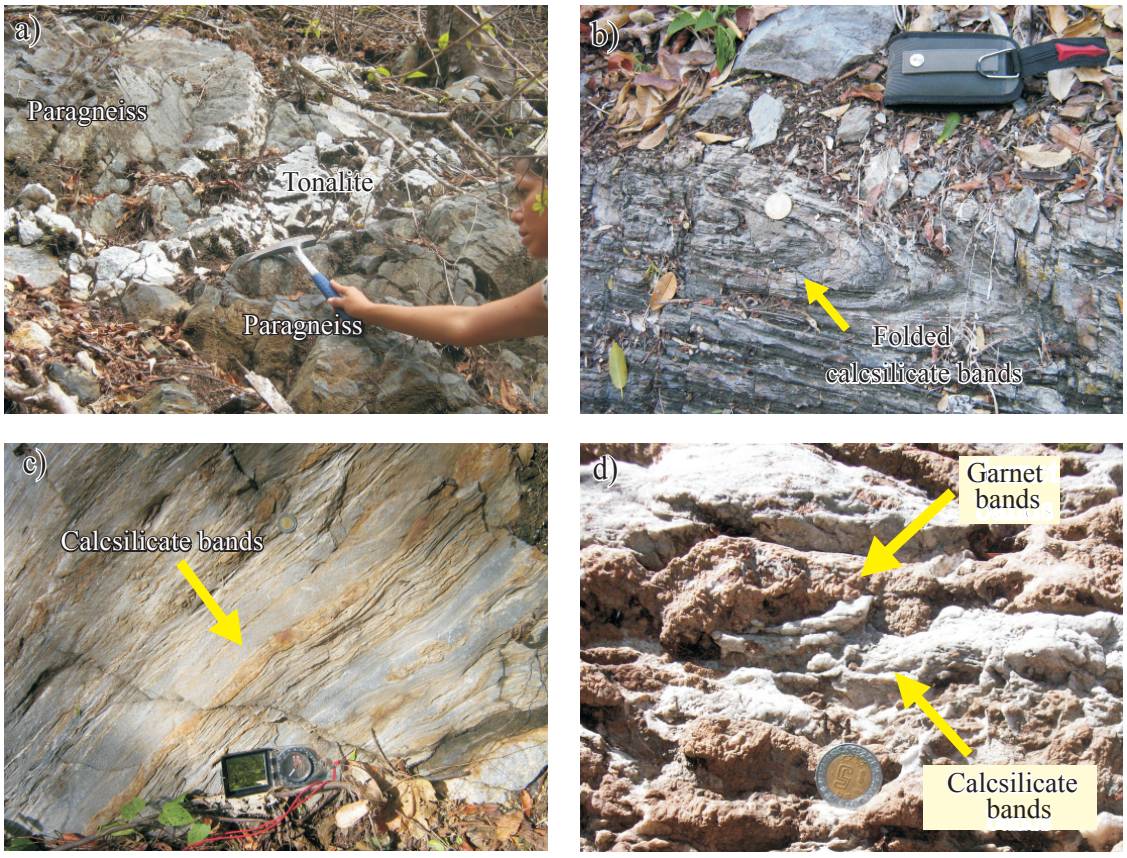

Figure 4. Metasedimentary rocks exposed in the Papelillo canyon. a) Garnet-bearing paragneiss in contact with a tonalitic body. b) Folded calcsilicates affected by contact metamorphism. c) Folded and banded calcsilicate rocks. d) Calcsilicate rocks with garnet bands.

large parts of the island. Undeformed granites, granodiorites, and tonalites (lithologies from petrographical observations) are the most abundant plutonic rocks, and some minor hypabyssal bodies and dikes also occur.

Abundant outcrops of granodioritic-tonalitic rocks are exposed along a 7 km transect between the northwestern coast and Papelillo (Figure 5a, 5b). Two main normal fault systems with dips to the NW (331°/62°) and SW (266°/40°) are affecting these rocks, which are massive and heterogeneous bodies with coarse- to medium-grained textures, with aplitic and pegmatitic dikes (Figure 5a). The latter are frequently emplaced along fault planes in the northwestern part (sample 0913, Figure 5b). The main mineral phases are zoned and twinned plagioclase, euhedral crystals of potassium feldspar with graphic and symplectitic textures, quartz, hornblende (sometimes replaced by chlorite and oxides), and biotite. Accessory phases are zircon, apatite, and occasionally euhedral sphene. In the Papelillo canyon, tonalitic-granodioritic rocks (sample 0911) intruded the metasedimentary unit (Figure 4a).

On the other hand, granites (*sensu strictu*) are abundant in the lower Papelillo canyon and along the southwestern coast (Figure 5c). As with the tonalites, the granites are affected by two normal fault systems that dip to the NW (312°/59°) and to the SW (256°/71°). The granites (samples 0932 and 1004) are massive, grey- to pink-colored, fine- to medium-grained, with granular textures, and are formed by potassium feldspar, quartz, and plagioclase. Accessory components are chlorite, biotite, opaque minerals, pyroxene, and secondary muscovite and epidote. Quartz is anhedral and potassium feldspar occasionally displays microcline twinning.

Granodiorites are found along the western coast, near the entrance to the Papelillo base camp. These rocks are exposed as a massive, light grey hypabyssal body (sample 0902, Figure 5d), with granophyric texture, formed by a microcrystalline matrix of quartz aggregates (enclosing larger crystals of anhedral quartz), potassium feldspar, twinned plagioclase, opaque minerals, and hornblende. Feldspars display sericitic alteration. In the Papelillo canyon, a NNE-SSW trending structure (Figure 2) seems to separate the granites from the other plutonic units previously presented.

Abundant outcrops of 10–250 m thick mafic dikes occur at the southern coast of Isla María Madre, close to Laguna del Toro (Figure 2). A group of these dikes was macroscopically classified as diabase (sample 1002, Figure 5e) with dark grey to greenish grey colors and aphanitic textures, affected by faults, fractures, and hydrothermal processes. Plagioclase crystals are subhedral, show albite twinning, are partly sericitized, and are set in a fine-grained matrix of hornblende and pyroxene. Chlorite and oxides partly replace hornblende.

Along the road from Laguna del Toro to Papelillo, a large hydrothermally altered mafic dike is exposed (sample 0901, Figure 5f) with grey to greenish colors and a porphyric texture. Recognized mineral phases are plagioclase and amphibole, frequently replaced by chlorite. Other second-

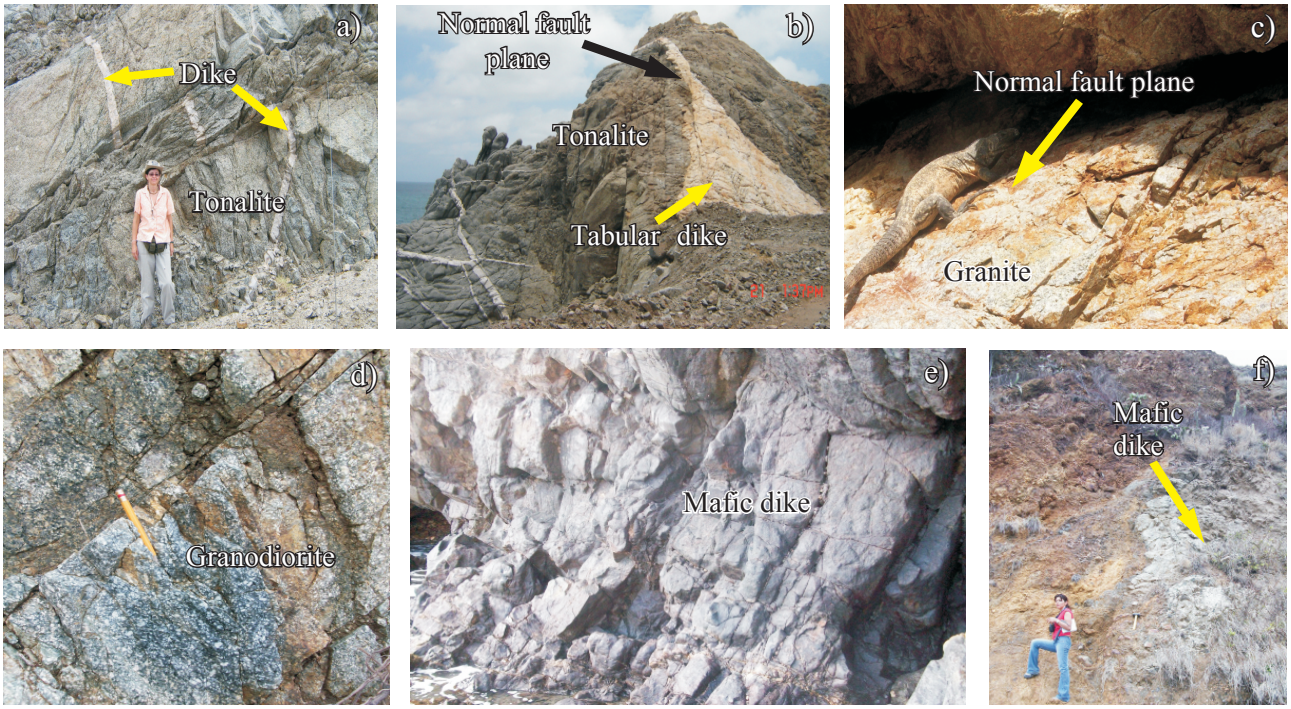

Figure 5. Plutonic rocks. a) Tonalitic rocks cut by pegmatitic dikes at the western coast of Isla María Madre. b) Pegmatitic tabular dike in a tonalitic body. c) Granitic rocks exposed along the southwestern coast of Isla María Madre. d) Hypabyssal granodiorite at the southern entrance of the Papelillo canyon. f) Diabase dike south of Laguna del Toro. e) Altered mafic dike SW of Laguna del Toro.

ary phases are epidote, chalcopyrite, and opaque minerals in a silicic microcrystalline groundmass. Hydrothermal processes have often destroyed the original textures of these rocks, which probably represent the youngest magmatic event in the island.

Volcanic rocks and several sedimentary sequences overlie the metamorphic and plutonic rocks.

Rhyolitic volcanic rocks

Volcanic rocks are broadly distributed in the western and central part of the island and they are mainly of rhyolitic composition (Figure 2; Table 1). Three volcanic units are distinguished: 1) ignimbrites and breccias, 2) massive, undeformed lava flows, and 3) strongly fractured and faulted

Table 1. Modal mineralogical compositions of Isla María Madre rock units (1000 points counted).

Sample	Coordinates UTM	Unit	Rock type	Qz	Plg	K-Feld	Hbl	Px	Bt	Grt	Ox	Msv	Chl	Ep	Mx
0909	13 Q 334129 2389894	Basement	Paragneiss	59.5	2.4	9	-	-	22.2	7	-	-	-	-	-
0915	13 Q 331273 2389851	Basement	Orthogneiss	52.2	12.6	24.3	-	-	10.1	-	-	0.8	-	-	-
0916	13 Q 331273 2389851	Basement	Orthogneiss	41	4	35	-	-	13	-	-	7	-	-	-
0936	13 Q 331598 2390168	Basement	Orthogneiss	42.3	28.5	8.7	-	-	18.8	-	0.7	0.2	0.7	-	-
0939	13 Q 331472 2390163	Basement	Orthogneiss	38.2	4.2	27.1	-	-	12.6	16.1	0.2	1.6	-	-	-
0940A	14 Q 331472 2390163	Basement	Orthogneiss	43.7	8.3	14.3	2.9	-	26.7	-	3	1.1	-	-	-
0902	13 Q 333369 2388301	Plutonic	Granodiorite	39.4	16.1	23.1	11.8	-	-	-	3.2	-	3.2	3.2	-
0907	13 Q 334356 2390116	Plutonic	Tonalite	18.2	51.5	4.9	12.9	-	11.2	-	0.3	-	0.9	-	-
0911B	13 Q 334030 2389415	Plutonic	Tonalite	14.4	47.1	11.2	10.7	-	16.4	-	0.2	-	-	-	-
0914	13 Q 331740 2389184	Plutonic	Tonalite	12	52.8	17	10.2	-	8	-	-	-	-	-	-
0932	13 Q 335277 2387118	Plutonic	Granite	20.6	21.8	53.3	-	0.4	0.1	-	1.2	2	-	-	-
1004	13 Q 339293 2385434	Plutonic	Granite	36	26	30	-	-	2	-	-	-	6	-	-
0904	13 Q 336094 2391779	Volcanic	Rhyolite	10	3.2	12.8	-	-	-	-	2.4	-	-	-	71.6
0905	13 Q 335569 2391820	Volcanic	Trachydacite	10	2.4	15.2	-	1.4	-	-	2.8	-	-	-	68.2
0920	13 Q 329663 2396208	Volcanic	Rhyolite	25	2	20	-	-	-	-	7	-	-	-	46
0933B	13 Q 333695 2389120	Volcanic	Rhyolitic Breccia	2.1	5	22.5	1.4	0.2	-	-	2.7	0.6	1.4	-	64
0945A	13 Q 336447 2396601	Volcanic	Rhyolite	6.6	1.6	8	1	1.2	-	-	1.2	0.2	-	1	79.1
0951B	13 Q 329785 2394659	Volcanic	Trachyte	0.7	1.1	12.8	-	-	-	-	0.9	-	3.7	0.4	80.4
1001	13 Q 343170 2386210.75	Volcanic	Rhyolite	19	9	28	-	-	-	-	6	-	-	-	38
LAH	13 Q 333439 2396593	Volcanic	Trachyte	0.2	1.2	7	-	0.8	-	-	3.5	-	-	6.1	81.3
1010	13 Q 346829 2376122.86	Volcanic	Rhyolit	5	17	16	-	-	-	-	0.3	-	-	0.9	60.8
0901	13 Q 339972 2385513	Mafic Dike	Mafic Dike	-	3.2		-	-	-	-	-	-	49.4	18.8	28.6
1002	13 Q 339594 2385307	Diabase Dike	Diabase Dike	-	13.2	8.8	3.7	-	-	-	1.2	-	2.3	3.9	66.9

Mineral abbreviations: Qz= Quartz, Plg= Plagioclase, K-Feld= Potassium feldspar, Hbl= Hornblende, Px= Pyroxene, Grt= Garnet, Ox= Oxides, Msv= Muscovite, Chl= Chlorite, Ep= Epidote, Mx= Matrix.

Figure 6. Volcanic rocks. a) Massive and altered ignimbrite unit exposed in the northwestern part of the island. b) Normal fault plane that separates tonalites from a massive volcanic breccia in the Papelillo canyon. c) Faulted and fractured rhyolite near Laguna del Toro. d) Rhyolite discordantly covering granitic rocks near Camarón. e) Faulted and fractured rhyolite with hydrothermal veins near Camarón.

lava flows.

Ignimbrites occur in the central and northwestern parts of Isla María Madre and in the Papelillo canyon (Figure 6a). The most voluminous outcrops are exposed in the highest parts of the island between Microondas and El Mirador (Figure 2) in the form of reddish brown, banded rhyolites (sample 0905 and 0904). The texture is eutaxitic with a vitreous groundmass, quartz and potassium feldspar (sanidine) as major components, and rare plagioclase. Accessory phases are pyroxene, oxides, apatite, and zircon. Similar ignimbrites occur in the northwestern part of the island (*e.g.*, sample 0920). In the Papelillo canyon, ignimbrites are in contact with tonalites along a normal fault plane (sample 0933B; Figure 6b) that dips to the NE (021°/68°). The exposed rocks correspond to a massive, reddish brown pyroclastic (rhyolitic) breccia, composed of a vitreous groundmass, which contains some metamorphic lithics. Major mineral components are potassium feldspar, plagioclase, and quartz. Accessory phases are hornblende, pyroxene, opaque minerals, chlorite, sericite, apatite, and zircon.

Undeformed lava flows are exposed in two locations on the island: in the south-eastern part, south of El Mirador (Figure 2), massive rhyolitic lava flows of light grey color and eutaxitic texture are characterized by a vitreous matrix that contains sanidine phenocrysts, plagioclase, quartz, and alteration products such as epidote, sericite, and chlorite. Zircon, apatite and opaque minerals are present as accessory phases (sample 1010). A reddish to purple rhyolitic lava flow (sample 0945A) is exposed along the road that connects the Rehilete with Bugambilias camps. These rocks are massive, with porphyritic texture and a microcrystalline silicic groundmass with potassium feldspar, quartz, plagioclase, pyroxene, oxides, and hornblende, along with sericitic and chloritic alterations. This lava flow is strongly affected by hydrothermal alteration.

Strongly fractured and faulted volcanic rocks were observed in small areas along the western coast of Isla María Madre. South of Laguna del Toro, these rocks are affected by SW and SE oriented fault systems (sample 1001; Figure 6c). Sedimentary sequences cover the contact between the plutonic and the volcanic rocks, but field observations clearly indicate that the granitoid rocks underlie this volcanic unit. Near Camarón, these volcanic rocks are exposed as a lava flow covering the granite discordantly (Figure 6d). This unit is affected by two normal fault systems that dip to ENE (065°/62°) and NW (320°/50°). Along major fault planes, feldspar-rich, leucocratic hydrothermal veins were emplaced

(Figure 6e). These rocks display a porphyritic texture with a vitreous matrix that contains sanidine phenocrysts, as well as minor quartz, plagioclase, chlorite, epidote, and oxides (sample 0921). Due to intense hydrothermal alteration processes, the original composition of these rocks is difficult to constrain. Modally, they were classified as trachytes (Table 1), but geochemical data suggest rhyolitic compositions.

Sedimentary rocks

The most widespread rocks in Isla María Madre are sedimentary sequences of marine and continental origin that are informally grouped into the Isla Magdalena sandstone and Ojo de Buey sequence.

Clastic sedimentary rocks (Isla Magdalena sandstone)

Exposures of sandstone strata in the southern part of Isla María Madre (Figure 7a) are correlated in this work to a sedimentary sequence observed in the neighboring María Magdalena Island, and is designated here as Isla Magdalena sandstone. In María Madre, these rocks crop out at the beach section located south of Laguna del Toro (sample 1003; Figure 2). Strata planes dip to the NE (70°/28°) and the overall sequence is affected by normal faults that dip to the SW (148°/80°, Figure 7b). The sandstones show terrigenous components such as quartz, potassium feldspar, plagioclase and minor calcite, biotite, and chlorite as well as some reworked foraminifera fragments in a silicic and slightly consolidated clay matrix. Hydrothermal processes (Figure 7c) affect the western segment of these sedimentary rocks.

Ojo de Buey sequence

Due to its characteristic type locality, we named a group of sedimentary sequences, studied previously by Carreño (1985) and McCloy *et al.* (1988), as "Ojo de Buey" sequence (Figure 8a). These authors investigated in detail three specific sections in the NE part of the island called Balleto Road, Playa Caleras, and Arroyo Hondo (Figure 2). In this work, we divided the Ojo de Buey sequence according to its deformation structures and stratigraphic position into 1) lower Ojo de Buey sequence and 2) upper Ojo de Buey sequence (Figure 8b).

Marine strata of the lower Ojo de Buey sequence crop out mostly in the northeastern part of the island. Along the northern coast (Figure 2), it is folded and affected (Figure 8b and c) by two normal major fault systems that dip 033°/42° NE and an inverse fault system that dips 029°/59° NE. It is composed of fine- to medium-grained, sandstone with quartz, plagioclase, potassium feldspar, minor biotite, chlorite, epidote, and scarce fragments of reworked foraminifera (sample 0917). All these components are sparite-cemented

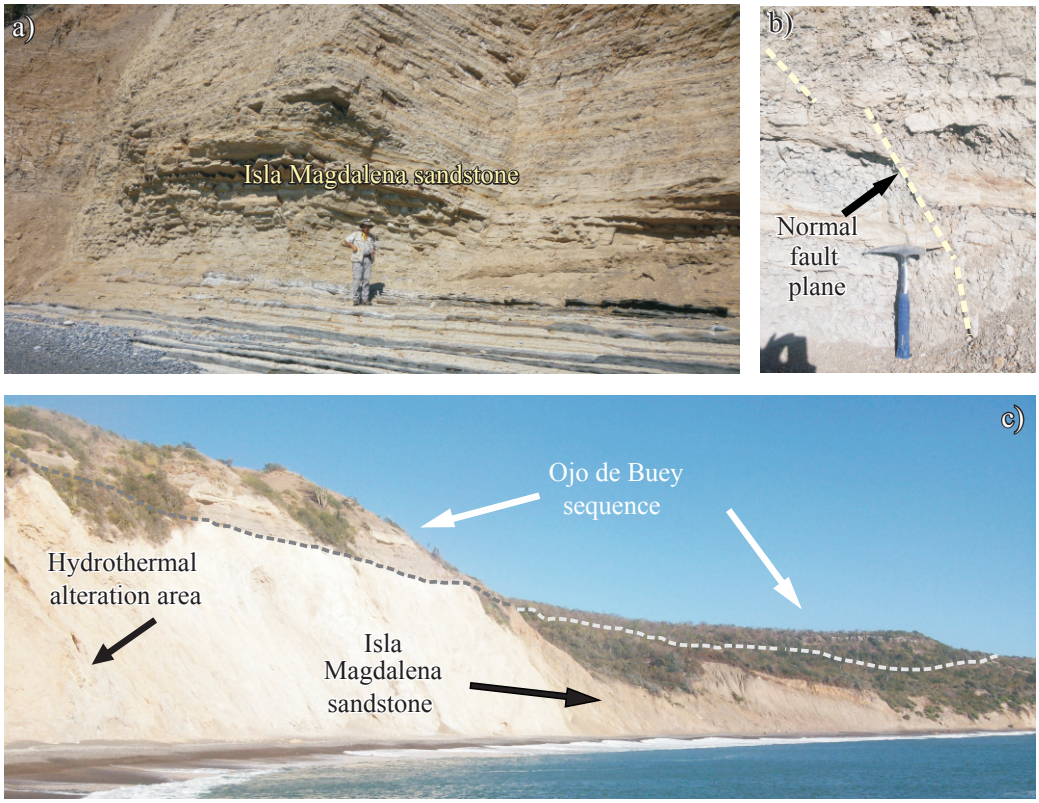

Figure 7. a) Clastic sequence (Isla Magdalena sandstone) south of Laguna del Toro. b) Normal fault affecting the sequence. c) Stratigraphic relation between the Isla Magdalena sandstone (bottom) and the Ojo de Buey sequence (top) along the southern María Madre coast.

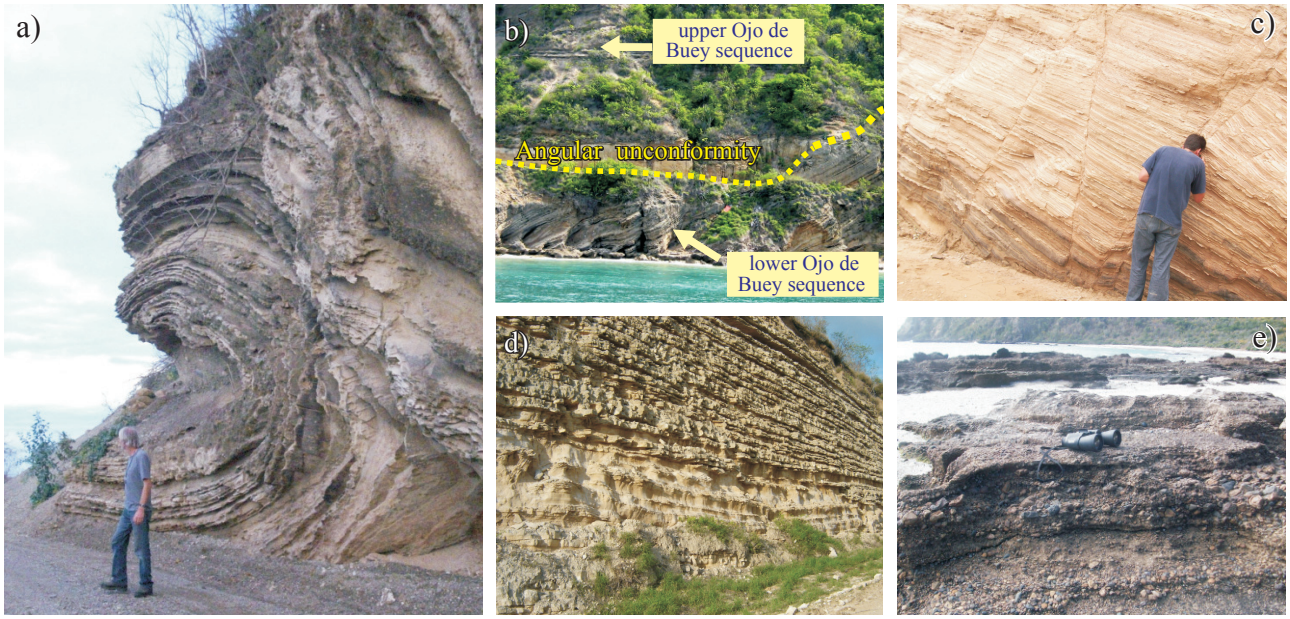

Figure 8. Sedimentary rocks. a) Ojo de Buey fold structure at the type location. b) Contact of the upper and lower Ojo de Buey sequence at the northeastern part of Isla María Madre. c) Fault planes observed in the lower Ojo de Buey sequence near Caleras Beach. d) Upper Ojo de Buey sequence on unpaved road from Balleto to Aserradero. e) Polymictic conglomerate of the upper Ojo de Buey sequence at the southern part of the island.

and show some intercalated carbonaceous horizons. This part of the unit can be correlated with the sequence exposed on the road from Caleras Beach to Arroyo Hondo (McCloy *et al.*, 1988). In the Caleras Beach section (Figure 2; Carreño, 1985), strata are composed of a light brown to white, folded, micritic-cemented limestone formed by clamshells and bioclasts with fragments of foraminifera, bryozoans, mollusks, red algae, echinoderms, and minor biogenic silica (sample 0948). The contact between the lower Ojo de Buey sequence and the overlying upper Ojo de Buey sequence is exposed as an angular unconformity (Figure 8b).

Outcrops of the upper Ojo de Buey sequence are mainly located along the eastern and southern coasts of the island and consist of light brown, medium-grained sandstone (Figure 8d) that dips gently to the NW (296°/12°). Strata are made up by mid to lower bathyal sandstone, siltstone and foraminiferous limestone (McCloy *et al.* 1988). Along the unpaved road from Balleto to Aserradero, micrite-sparite cemented fine-grained sandstones (sample 0944) are gently folded with strata that dips to the SW (091°/10°). This sequence is formed by quartz, plagioclase, sanidine, biotite, altered amphibole, and oxides together with minor foraminifera fragments. Occasionally, ash layers were observed in this unit.

Further to the south, at Delfines beach, near Laguna del Toro, a coarse grained, well-sorted and indurated polymictic conglomerate forms part of the Upper Ojo de Buey sequence (Figure 8e). The clasts are of volcanic rocks and subordinate plutonic and metamorphic components, supported by a micrite-cemented sandy matrix with the occurrence of reworked fragments of foraminifera (sample 0929) as well as mollusks and gasteropods. Chiñas (1963) assigned a Plio-Pleistocene age to these rocks.

In comparison to the Isla Magdalena sandstone, the Ojo de Buey sequence present limestone horizons, biogenic silica, and minor detrital components.

GEOCHEMISTRY

Geochemical, isotopic and petrological aspects of Islas Marías rocks will be discussed in detail in a forthcoming paper, but some preliminary geochemical data of igneous and metamorphic units from Isla María Madre are presented here as an overview.

Analytical procedures

Sampling locations are shown in Figure 2 and coordinates are given in supplementary Table A1. Only fresh rocks were processed by crushing in a jawbreaker, grinding in a roller mill, and pulverizing with a steel mill set. Analyses of major elements were performed for 35 samples by X-ray fluorescence spectrometry using a Siemens SRS-3000 instrument at the Laboratorio Universitario de Geoquímica Isotópica (LUGIS), Instituto de Geología, Universidad Nacional Autónoma de México (UNAM), according to the procedures described by Lozano-Santa Cruz and Bernal (2005). For 28 of these samples we obtained trace element data by Inductively Coupled Plasma Mass Spectrometry

(ICP-MS) (Table A1) using a Thermo Series XII instrument at the Centro de Geociencias (CGEO), Juriquilla, UNAM, following the sample preparation and measurement procedures described by Mori *et al.* (2007).

Basement and plutonic rocks

Six orthogneiss samples of granodioritic to granitic composition (SiO_2: 61.6 – 75.0 wt.%, Table A1), a biotite-garnet-paragneiss (sample 0909; SiO_2: 67.4 wt.%), and a biotite-paragneiss (sample 0912; SiO_2: 62.3 wt.%) from the metamorphic basement were analyzed. Nine plutonic rocks, including a pegmatitic dike (sample 0941), have dioritic, tonalitic, granodioritic, and granitic compositions (SiO_2 56.2–71.7 wt.%) in the total alkali *vs.* silica diagram (TAS; Cox *et al.*, 1979, Figure 9a) . Most rocks plot in the sub-alkalic field, with the exception of a leucocratic, nearly aplitic alkaline granite (sample 0932), which shows sericitic and chloritic alterations. Mafic dikes and inclusions (samples 0901, 0923, 0924A, 0952, and 1002) generally show gabbroic compositions. With respect to trace elements, 13 intrusive rocks (granite, granodiorite, tonalite, and mafic dikes) plot in the subduction-related Volcanic-Arc-Granite field in the Y+Nb *vs.* Rb discrimination diagram (Figure 9b; Pearce *et al.*, 1984). Chondrite-normalized rare earth element (REE) patterns for these samples show enrichment for Light REE, frequently seawater derived negative Ce anomalies, and the presence (granite 0932 and pegmatitic dike 0913) or absence (0914 and 0902) of negative Eu anomalies (Figure 9c). The latter corresponds to tonalite and granodiorite samples with obviously less magmatic differentiation with respect to the granite and pegmatitic dike samples. The overall REE spectrum is typical for subduction related continental arc granites. The Laguna del Toro mafic dike (sample 0901; Figure 2) shows less enriched LREE concentrations and no negative Eu anomaly, common in less evolved magmas.

Rhyolitic volcanic rocks

Nine volcanic rocks were analyzed for major elements and additional trace element data were obtained for seven

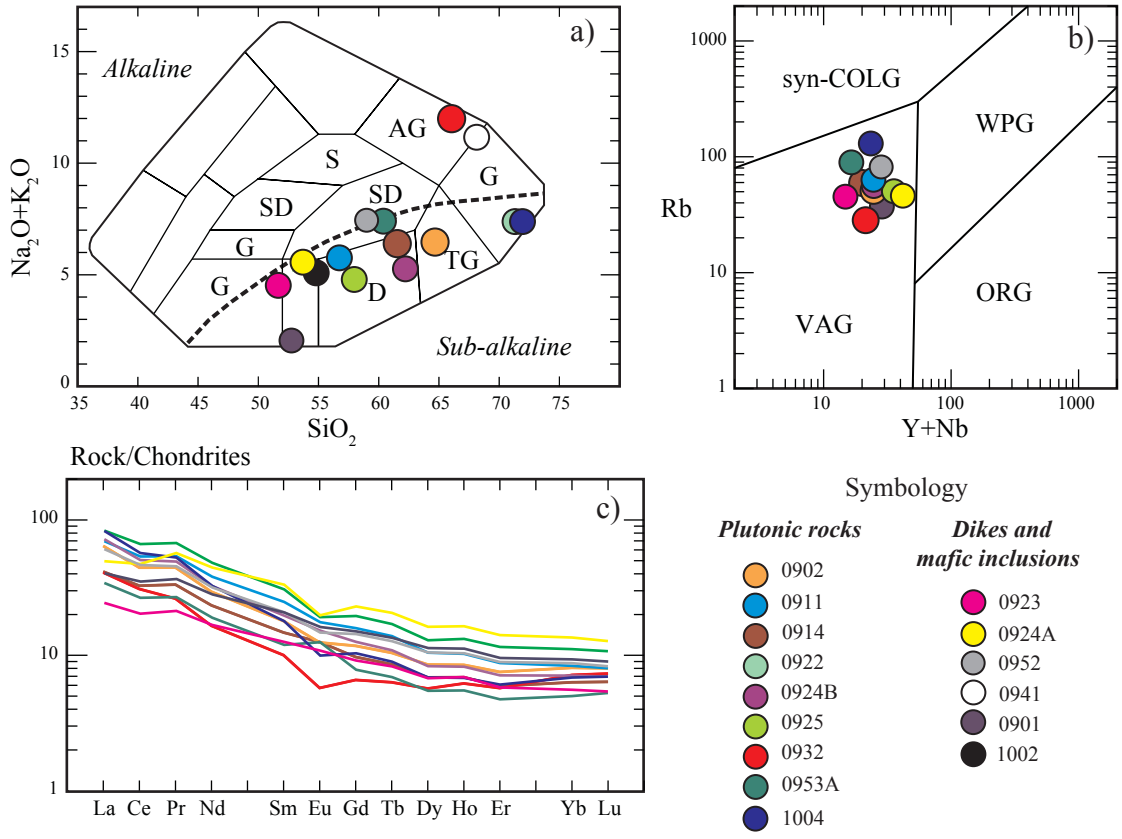

Figure 9. a) Total Alkali *vs.* Silica (TAS) diagram (normalized values; modified from Cox *et al.*, 1979) for the chemical classification of plutonic rocks. AG = Alkaline Granite; G = Granite; S = Syenite; SD Syenite-Diorite; G = Gabbro; D = Diorite; TG = Tonalite-Granodiorite. b) Tectonic discrimination diagram for plutonic rocks (Pearce *et al.*, 1984). VAG = volcanic arc granites; WPG = within plate granite; ORG = ocean-ridge granites; syn-COLG = syn-collisional granites. c) Chondrite normalized REE patterns for María Madre plutonic rocks (Nakamura, 1974). Samples 0941 and 1002 were only analyzed for major elements.

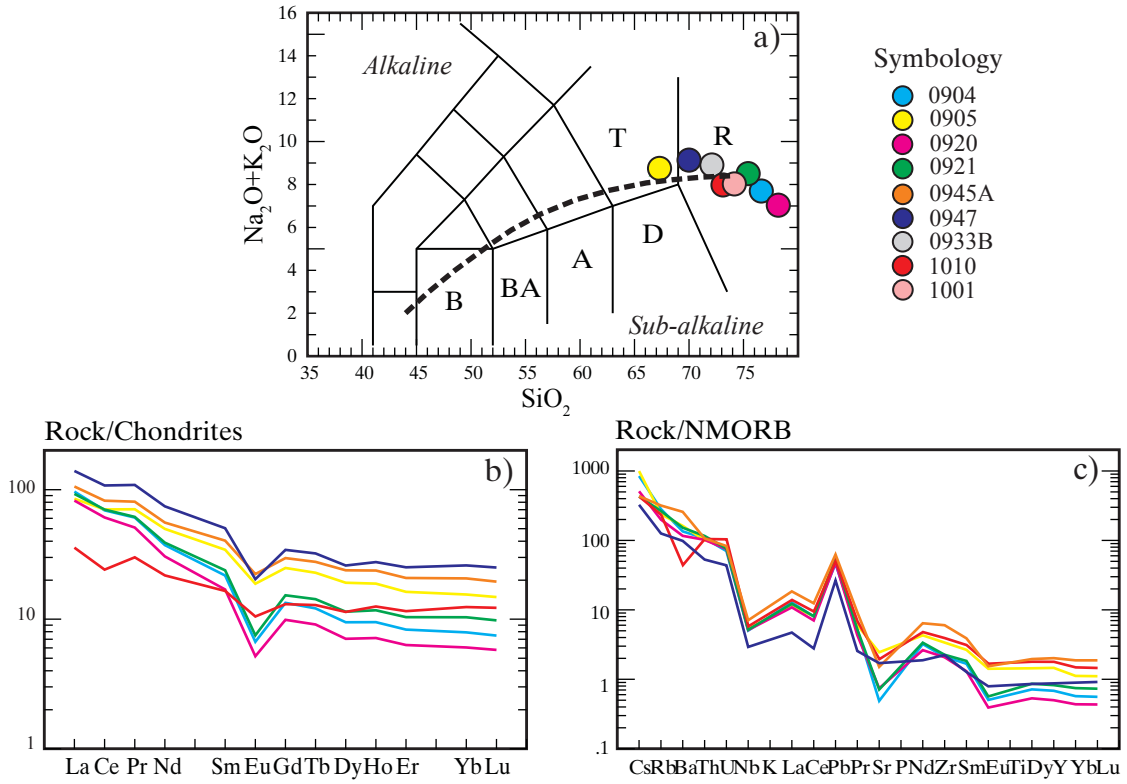

Figure 10. a) Total Alkali *vs.* Silica (TAS) diagram (normalized values; Le Bas *et al.*, 1986) for the chemical classification of volcanic rocks. B = Basalt; BA = Basaltic Andesite; A = Andesite; D = Dacite; R = Rhyolite; T = Trachyte. b) Chondrite normalized REE diagram for volcanic rocks (Nakamura, 1974). c) NMORB normalized spider diagram for Isla María Madre volcanic rocks (Sun and McDonough, 1989). Sample 1001 was analyzed only for major elements and sample 0945A was excluded in the TAS diagram due to intense hydrothermal alteration.

of these rocks (Table A1). In general, the Isla María Madre volcanic sequence is composed of rhyolitic rocks (SiO_2 between 61.6 and 76.7 wt.%), with the exception of one trachydacite (Table A1; Figure 10a). Since rhyolite sample 0945A shows influence of hydrothermal alterations, it was not plotted in the TAS diagram of Figure 10a.

The REE patterns of the analyzed volcanic rocks are shown in Figure 10b. They display strongly fractionated LREE, similar to the plutonic suite (Figure 10c) but with more pronounced negative Eu anomalies. The NMORB-normalized spidergram of Figure 10c shows typical subduction regime patterns with considerable enrichments for Large Ion Lithophile Elements (LILE) such as Cs, Rb, Ba, and Pb in comparison to High Field Strength Elements (HFSE; *e.g.*, Nb, Ti, Zr) and P, which are partly incorporated into the fractionation assemblage.

GEOCHRONOLOGY

Analytical procedures

U-Pb analyses

For age determinations with the U-Pb method, we selected zircons from a total of seven samples, including two gneisses (0915 and 0916), two plutonic rocks (0911B and 0932), two sandstones from the Ojo de Buey sequence (0917B and 0948) and a sample from the Isla Magdalena sandstone, south of Laguna del Toro (1003). Sample locations are shown in Figure 2 and Table A1. The rocks were crushed, milled and sieved, and zircons were separated from the <80 mesh fraction by standard procedures at LUGIS-UNAM, by using a Wilfley® table or a gravitational zircon separation technique, a Frantz® isodynamic separator, heavy liquids, and handpicking techniques.

U-Pb geochronology of zircons was conducted by laser ablation multicollector inductively coupled plasma mass spectrometry (LA-MC-ICPMS) at the Arizona LaserChron Center (Gehrels *et al.*, 2008). The analyses involve ablation of zircon with a Photon Machines Analyte G2 Excimer laser (samples 0911B, 0915, 0916, and 1003) or a New Wave UP193HE Excimer laser (samples 0932, 0917B, and 0948) using a spot diameter of 30 microns. The ablated material is carried in helium into the plasma source of a Nu HR ICPMS, which is equipped with a flight tube of sufficient width in order to analyze U, Th, and Pb isotopes simultaneously. All measurements are made in static mode, using Faraday detectors with 3×10^{11} Ohm resistors for ^{238}U, ^{232}Th, ^{208}Pb-^{206}Pb, and discrete dynode ion counters for ^{204}Pb and ^{202}Hg. Each analysis consisted of one 15-second integration on

peaks with the laser off (for backgrounds), 15 one-second integrations with the laser firing, and a 30-second delay to purge the previous sample and prepare for the next analysis.

For each analysis, the errors in determining $^{206}Pb/^{238}U$ and $^{206}Pb/^{204}Pb$ result in a measurement error of ~1–2% (at 2-sigma level) in the $^{206}Pb/^{238}U$ age. The errors for $^{206}Pb/^{207}Pb$ and $^{206}Pb/^{204}Pb$ also result in ~1–2% (at 2-sigma level) uncertainty in age for grains that are >1.0 Ga, but are substantially larger for younger grains due to low intensity of the ^{207}Pb signal.

The interference of ^{204}Hg on ^{204}Pb was accounted for by measuring ^{202}Hg during laser ablation and subtraction of ^{204}Hg according to the natural $^{202}Hg/^{204}Hg$ ratio of 4.35. This Hg correction is not significant for most analyses because the Hg backgrounds are low (generally ~150 counts per second at mass 204).

Common Pb correction was accomplished by using the Hg-corrected ^{204}Pb and assuming an initial Pb composition from Stacey and Kramers (1975). Uncertainties (total values) of 1.5 for $^{206}Pb/^{204}Pb$ and 0.3 for $^{207}Pb/^{204}Pb$ are applied to these compositional values based on the variation in Pb isotopic composition in modern crystalline rocks.

Inter-element fractionation of Pb/U is generally ~5%, whereas apparent fractionation of Pb isotopes is generally <0.2%. In-run analyses of fragments of a large zircon crystal (generally every fifth measurement) of a known age of 563.5 ± 3.2 Ma (2-sigma error) were used to correct for this fractionation. The uncertainty resulting from the calibration correction is generally 1–2% (2-sigma) for both $^{206}Pb/^{207}Pb$ and $^{206}Pb/^{238}U$ ages. Concentrations of U and Th were calibrated relative to a Sri Lanka zircon standard, which contains ~518 ppm of U and 68 ppm Th.

The analytical data are reported in supplementary Table A2. Uncertainties shown in this table are at the 1-sigma level, and include only measurement errors.

The resulting interpreted ages are shown on Pb*/U concordia diagrams and weighted mean diagrams (igneous and metaigneous rocks) or relative age-probability diagrams (detrital zircons) using the routines in Isoplot (Ludwig, 2008). The weighted mean diagrams show the weighted mean (weighting according to the square of the internal uncertainties), the uncertainty of the weighted mean, the external (systematic) uncertainty that corresponds to the ages used, and the final uncertainty of the age (determined by quadratic addition of the weighted mean and external uncertainties).

$^{40}Ar/^{39}Ar$ analyses

For $^{40}Ar/^{39}Ar$ analysis, we selected four volcanic rocks (0921, 1010, 0904, and 0905) that were crushed and sieved. From these units sanidine crystals were separated using a Frantz® isodynamic separator and heavy liquid techniques at LUGIS-UNAM. Subsequently the samples were submitted to the Geochronology Laboratory at the University of Alaska in Fairbanks, where they were further purified. The monitor mineral MMhb-1 (Samson and Alexander, 1987) with an age of 513.9 Ma (Lanphere and Dalrymple, 2000) was used to monitor the neutron flux (and to calculate the irradiation parameter *J*). Samples and standards were wrapped in aluminum foil and loaded into aluminum cans of 2.5 cm diameter and 6 cm height. The samples were irradiated in position 5c of the uranium enriched research reactor of McMaster University in Hamilton, Ontario, Canada, for 20 Megawatt-hours. Upon their return from the reactor, the samples and monitors were loaded into 2 mm diameter holes in a copper tray that was then loaded in an ultra-high vacuum extraction line. The monitors were fused and samples heated, using a 6-Watt argon-ion laser, following the technique described in York *et al.* (1981), Layer *et al.* (1987) and Layer (2000). Argon purification was achieved using a liquid nitrogen cold trap and a SAES Zr-Al getter at 400°C. The samples were analyzed in a VG-3600 mass spectrometer at the Geophysical Institute, University of Alaska, Fairbanks. The measured argon isotope ratios were corrected for system blank and mass discrimination, as well as calcium, potassium and chlorine interference

Table 2. $^{40}Ar/^{39}Ar$ interpretive details.

Sample	Mineral	Integrated age (Ma)	Plateau age (Ma)	Plateau information	Isochron age (Ma)	Isochron or other information
0904	Sanidine	75.9 ± 1.5	**76.6 ± 1.4**	10 of 11 fractions 96.8 % ^{39}Ar release MSWD =0.6	77.6 ± 3.0	10 of 11 fractions $^{40}Ar/^{36}Ar_i$ = 295.2 ± 2.7 MSWD = 0.67
0905	Sanidine	80.6 ± 2.0	**80.6 ± 1.6**	5 of 11 fractions 82.9 % ^{39}Ar release MSWD = 1.0	81.2 ± 1.7	7 of 11 fractions $^{40}Ar/^{36}Ar_i$ = 293.1 ± 35.1 MSWD = 1.0
0921	Sanidine	55.5 ± 2.5	**55.4 ± 2.4**	10 of 11 fractions 98.0 % ^{39}Ar release MSWD = 1.12	57.7 ± 3.7	11 of 11 fractions $^{40}Ar/^{36}Ar_i$ = 295.3 ± 2.8 MSWD = 0.4
1010	Sanidine	82.6 ± 3.3	**71.6 ± 1.9**	7 of 9 fractions 53.7 % ^{39}Ar release MSWD = 2.28	63.0 ± 5.1	7 of 9 fractions $^{40}Ar/^{36}Ar_i$ = 302.2 ± 3.2 MSWD = 2.59

Samples analyzed with standard MMhb-1 with an age of 513.9 Ma. Most robust age in bold. Plateau ages are shown in Figure 15. Errors are given as ± 1 sigma.

reactions following procedures outlined in McDougall and Harrison (1999). System blanks generally were 2×10^{-16} mol ^{40}Ar and 2×10^{-18} mol ^{36}Ar, which are 10 to 50 times smaller than fraction volumes. Mass discrimination was monitored by running both calibrated air shots and a zero-age glass sample. These measurements were made on a weekly to monthly basis to check for changes in mass discrimination.

A summary of the $^{40}Ar/^{39}Ar$ results is given in Table 2, with all ages quoted to the ± 1 sigma level and calculated using the constants of Steiger and Jäger (1977). The integrated age is the age given by the total gas measured and is equivalent to a potassium-argon (K-Ar) age. The spectrum provides a plateau age if three or more consecutive gas fractions represent at least 50% of the total gas release and are within two standard deviations of each other (Mean Square Weighted Deviation less than ~2.5). Each sample was run twice to both confirm age determinations and to optimize analytical precision.

Results

U-Pb single zircon ages

The migmatitic orthogneiss (sample 0915) in the western part of Isla María Madre contains zircons with heterogeneous morphologies, including prismatic and medium-elongated crystals. The separated grains range from 50 to 300 µm in size (Figure 11a and 11b). A total of 36 zircon grains were analyzed (Table A2). Twenty concordant grains with apparent $^{206}Pb/^{238}U$ ages between 152 and 171 Ma yield a concordia age of 162.7 ± 2.9 Ma (95% confidence including 1.5% systematic error; Figure 11c), which is interpreted as the time of igneous protolith crystallization in the Middle Jurassic (Callovian). Concordant U-Pb data of two spots on zircon rims probably reflect the time of metamorphism between 83 and 87 Ma, whereas six spots with apparent $^{206}Pb/^{238}U$ ages from 116 to 145 Ma document either Pb-loss or zircon zones with mixed ages. Another eight laser spots contain varying amounts of inherited components yielding mostly discordant ages. The minimum ages of these spots, however, indicate inherited zircon components from late Mesoproterozoic to early Paleozoic sources.

A banded orthogneiss (sample 0916) was taken from the contact with the migmatitic orthogneiss described above. It contains short to medium sized prismatic and rounded crystals (Figure 12a and 12b). Twenty-four out of 35 analyzed laser spots on zircon grains are concordant with apparent $^{206}Pb/^{238}U$ ages between 164 and 175 Ma. The corresponding concordia age (Figure 12c) of 169.9 ± 2.9 Ma (95% confidence including 1.5% systematic error)

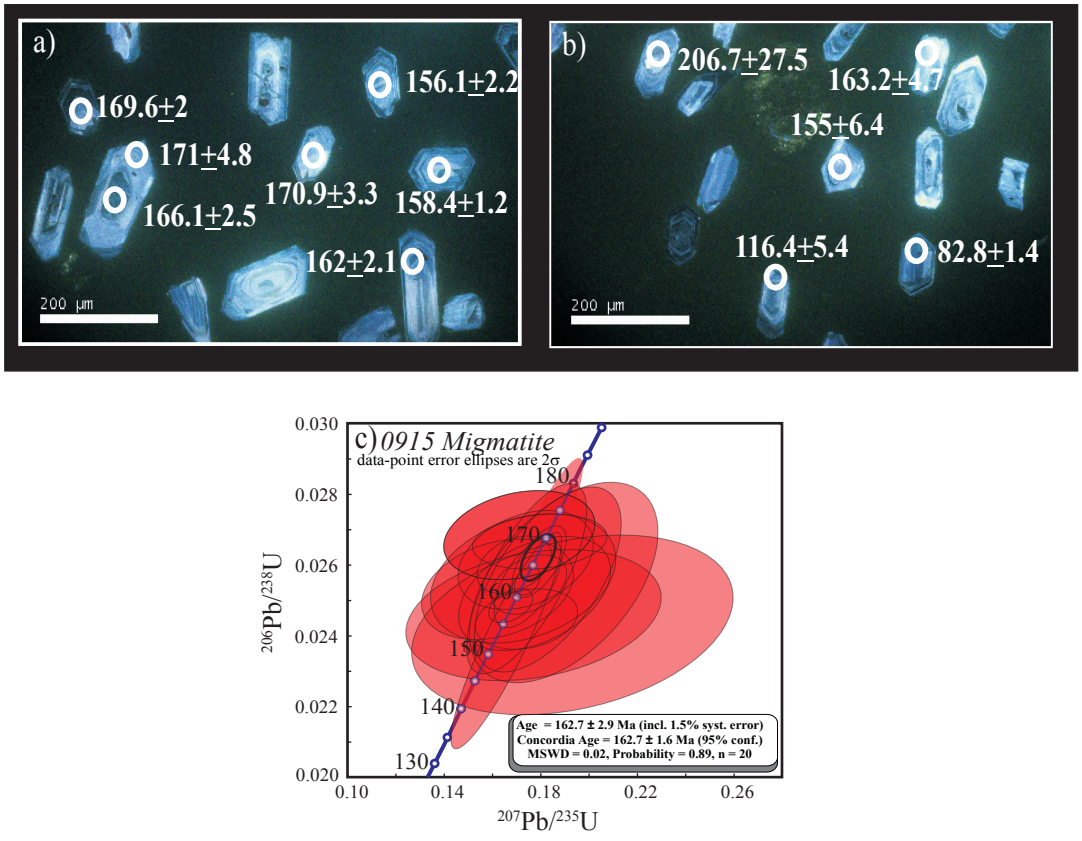

Figure 11. a) and b) Cathodoluminescence images and $^{206}Pb^*/^{238}U$ ages for selected laser spots on individual zircon grains from the migmatitic orthogneiss 0915. c) U-Pb concordia diagram of U-Pb isotope data of zircons from sample 0915. Error ellipses of individual spots are 2σ.

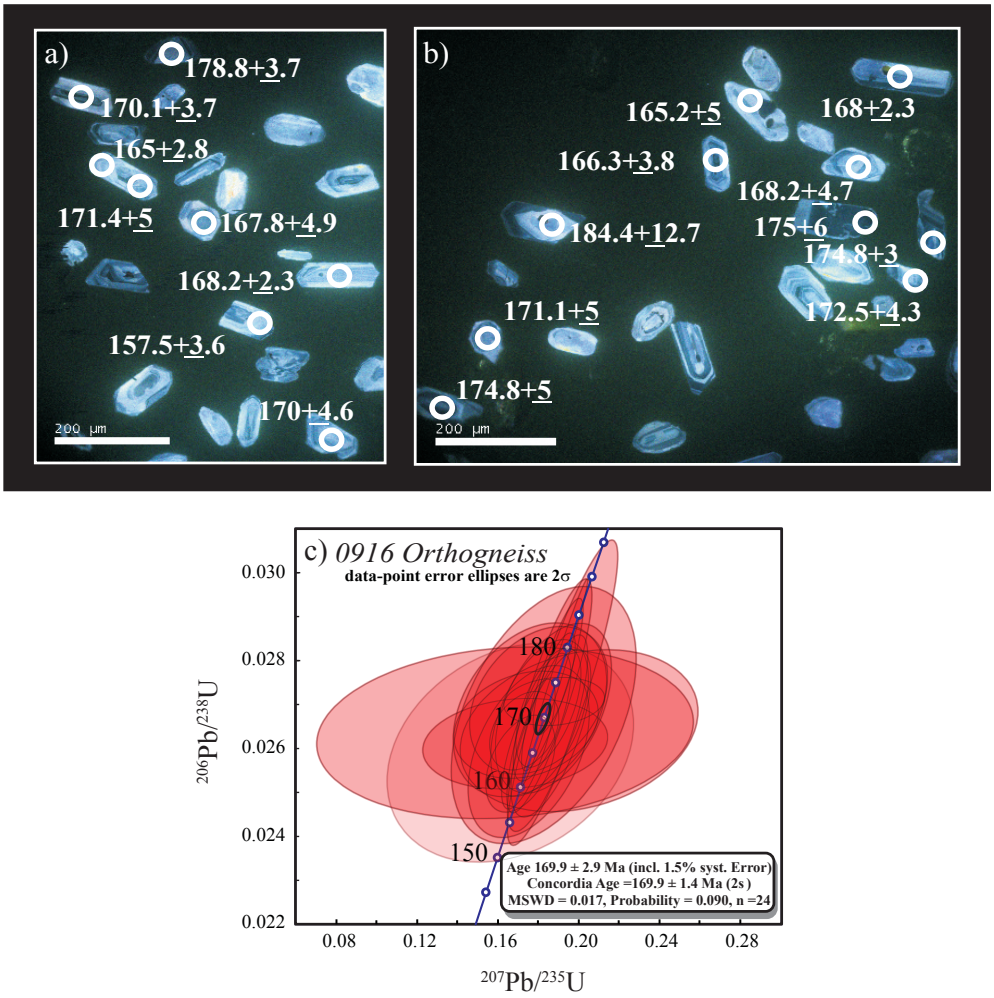

Figure 12. a) and b) Cathodoluminescence images and $^{206}Pb^*/^{238}U$ ages for selected laser spots on individual zircon grains from banded gneiss 0916. c) U-Pb concordia diagram showing U-Pb isotope data of zircons from sample 0916. Error ellipses of individual spots are 2σ.

is interpreted to reflect the time of igneous crystallization in the Middle Jurassic (Bathonian). The metamorphic event is documented by only one laser spot that yielded a concordant age of *ca.* 80 Ma. Discordant Mesoproterozoic and concordant Ordovician inherited zircon cores suggest assimilation of continental crust.

The concordia diagram for a tonalite (sample 0911B), that intrudes the metasedimentary sequence exposed in the Papelillo canyon, is shown in Figure 13a. The apparent $^{206}Pb/^{238}U$ ages of 22 analyzed spots range from 70.5 to 83.3 Ma. No older components were found. The crystallization age of this sample is interpreted from these 22 spots at $80.1^{+1.4}/_{-1.3}$ Ma (Campanian, Figure 13b) by using the TuffZirc algorithm (Ludwig and Mundil, 2002) and adding a systematic error of 1.5%.

The leucocratic granite 0932 was collected from the western coast between Laguna del Toro and Papelillo (Figure 2). Apparent $^{206}Pb/^{238}U$ ages of 27 analyzed spots range from 74.4 to 90.5 Ma (Figure 13c; Table A2). Another eight analyzed spots reflect inherited components yielding apparent $^{206}Pb/^{238}U$ ages from about 97 to 316 Ma. The crystallization age of this granite is interpreted from 23 spots at 84.2 $^{+3.1}/_{-2.5}$ Ma (calculated with TuffZirc algorithm, adding 1.9% of systematic error; Figure13d), which is within errors of the age of the tonalite 0911B.

Both granitoid rock ages are consistent with the ages obtained from metamorphic rims of the orthogneiss samples (see above).

A coarse to medium grained sandstone from the lower Ojo de Buey sequence (sample 0917B) was selected for detrital zircon provenance analyses. Sixty out of 65 analyzed zircon grains (Table A2) have Cretaceous $^{206}Pb/^{238}U$ ages between 68 and 121 Ma (Figure 14a). The most prominent peak in the relative probability distribution is at 83.4 Ma (Figure 14b), which is similar to the age obtained for the granitoids (Figure 13c, d). Another important group of 21 detrital zircons show Aptian-Albian ages from ~100 to ~121 Ma with two peaks at ~103 and ~111 Ma. The five remaining grains have Paleozoic and Mesoproterozoic ages from 249 to 451 Ma, and at 1282 and 1498 Ma (Table A2).

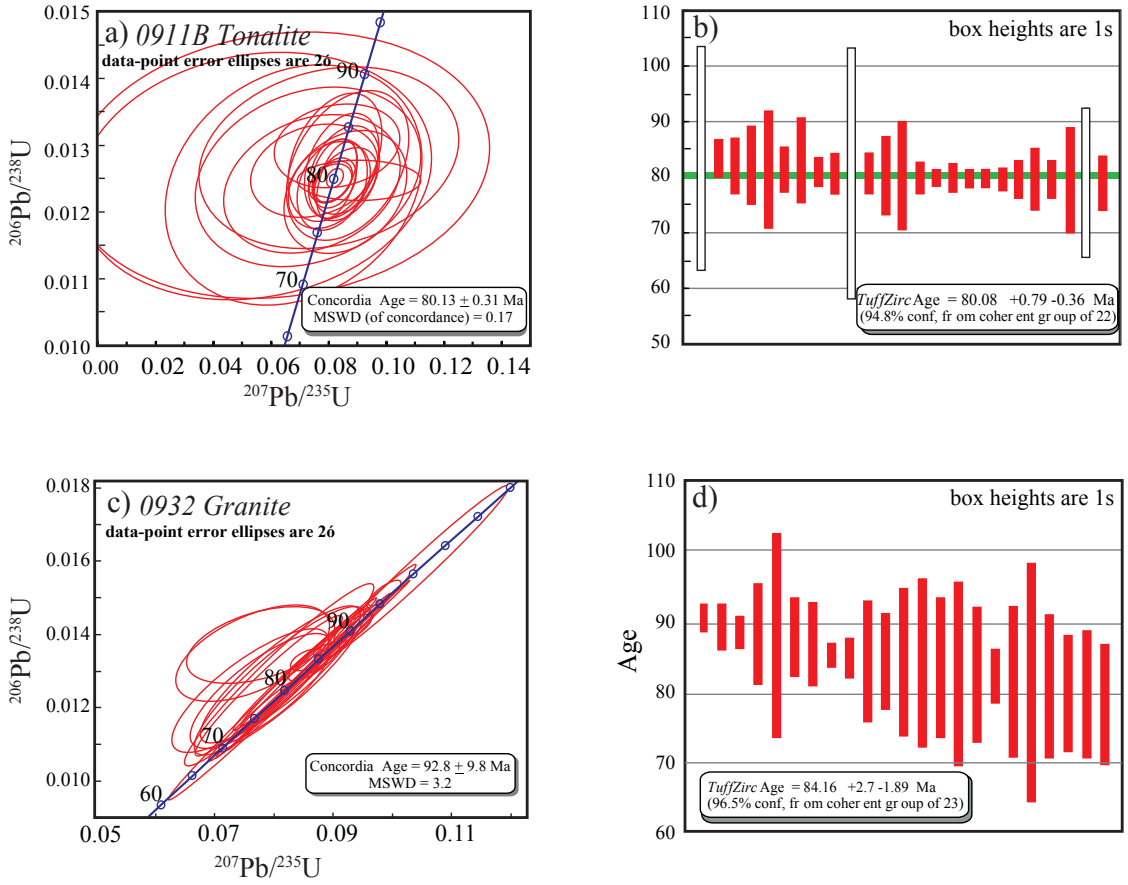

Figure 13. a) U-Pb concordia diagram displaying U-Pb isotope data of igneous zircons from tonalite sample 0911B. b) $^{206}Pb^*/^{238}U$ ages of 25 laser spots measured on igneous zircons. Note: Three samples (white boxes) were not included in age calculations. c) Concordia diagram of U-Pb isotope data of zircons from granite sample 0932. d) $^{206}Pb^*/^{238}U$ ages of 23 laser spots measured on igneous zircons from sample 0932.

From the overlaying upper Ojo de Buey sequence, a fine to medium-grained sandstone (sample 0948) was collected from the Arroyo Hondo Section (Carreño, 1985). Seventy-eight detrital zircon grains were analyzed and their isotopic ratios are plotted in a Tera-Wasserburg diagram (Figure 14c). Apparent $^{206}Pb/^{238}U$ ages of 73 zircon grains range from 70 to 100 Ma and define a prominent peak at *ca.* 83 Ma (Figure 14d), suggesting that the zircons in these sediments almost entirely originated from the Upper Cretaceous igneous rocks. The remaining five analyzed zircons document Aptian-Albian and Middle Jurassic sources.

A sandstone from the Isla Magdalena sandstone (sample 1003) was collected south of Laguna del Toro. Twenty-two out of 25 grains present Tertiary $^{206}Pb/^{238}U$ ages between 20 and 42 Ma (Figure 14e). The relative probability plot (Figure 14f) shows a prominent peak at 22 Ma and two minor peaks at 27 Ma and 34 Ma. In contrast to the Ojo de Buey sequence, only one zircon has an apparent Upper Cretaceous $^{206}Pb/^{238}U$ age of ~87 Ma. Based on field observations we suggest that this clastic unit forms part of the Isla Magdalena sandstone, a dominant sedimentary sequence of the homonymous island to the southeast

$^{40}Ar/^{39}Ar$ sanidine ages

$^{40}Ar/^{39}Ar$ geochronology was performed on sanidines from three rhyolites and a trachydacite of the Isla María Madre volcanic sequence. Results are summarized in Table 2 and the obtained age spectra are shown in Figure 15. Detailed analytical data is given in supplementary Table A3. Trachydacite (0905) and rhyolite (0904) samples correspond to the massive ignimbrites from the central and highest part of the island (Figure 2). The obtained plateau ages are 80.6 ± 1.6 Ma and 76.6 ± 1.4 Ma (1σ), respectively (Figura15a and b). Integrated ages (80.6 ± 2.0 Ma and 75.9 ± 1.5 Ma) and isochron ages (81.2 ± 1.7 Ma and 77.6 ± 3.0 Ma) are all within errors. From a rhyolitic lava flow sampled in the east-central part (sample 1010), a sanidine plateau age of 71.6 ±1.9 Ma was calculated (Figure 15c; intergrated age 82.6 ± 3.3 Ma; isochron age 63.0 ± 5.1 Ma). It is noteworthy, that these sanidine ages are comparable to the U-Pb zircon ages of the plutonic rocks, suggesting a contemporaneous or slightly younger magmatic event for the volcanic rocks, which is supported by field observations (Figure 6d).

From the fractured and deformed rhyolithic lava flow in the northwestern part of the island (sample 0921), a

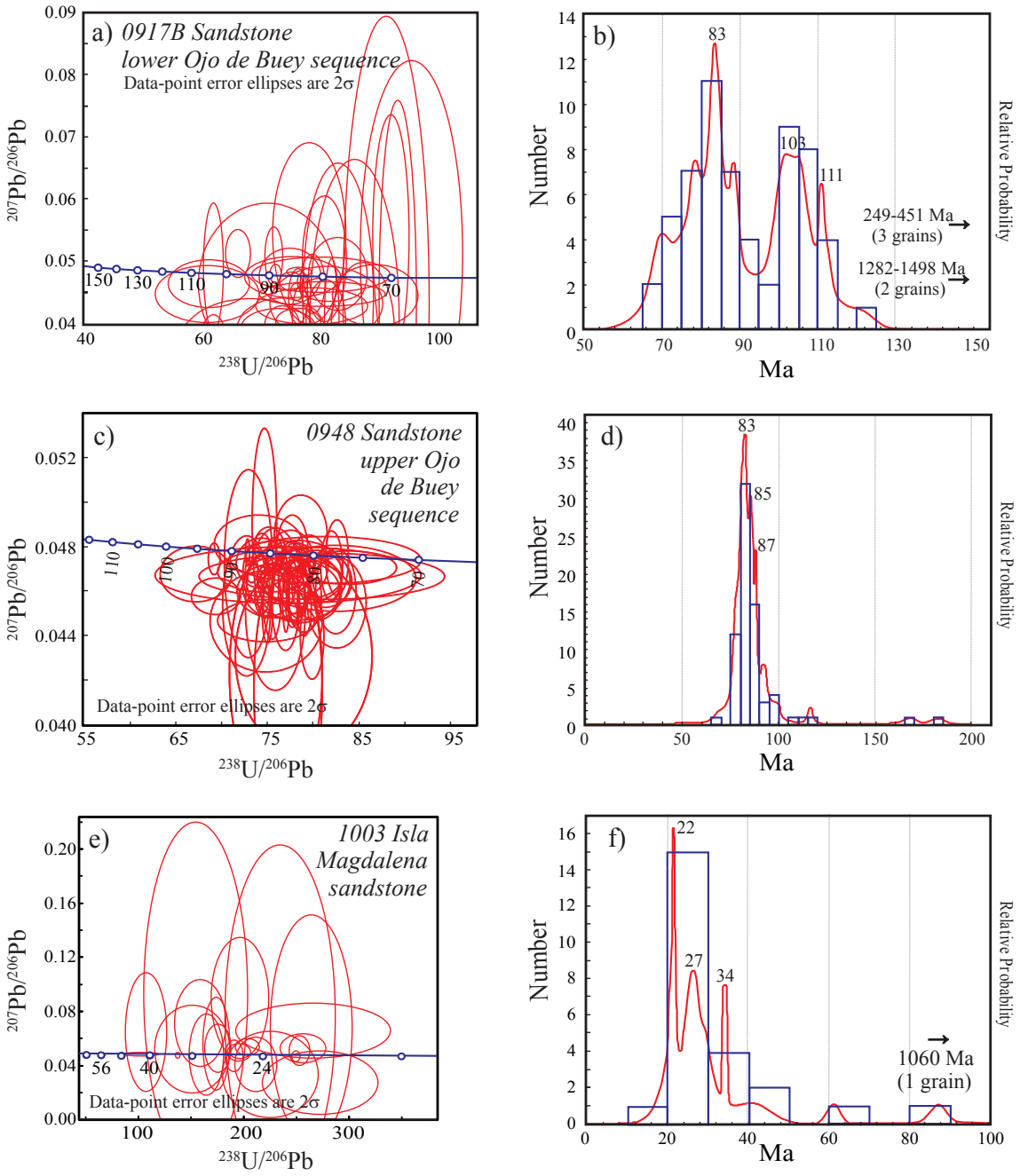

Figure 14. a) U-Pb Tera-Wasserburg diagram and b) relative probability and age histogram plot of zircon grains from sample 0917B (lower Ojo de Buey sequence). c) U-Pb Tera-Wasserburg diagram and d) relative probability and age histogram plot of zircon grains from sample 0948 (upper Ojo de Buey sequence). e) U-Pb Tera-Wasserburg diagram and f) relative probability and age histogram plot of zircon grains from sample 1003 (Isla Magdalena sandstone).

Lower Tertiary plateau age of 55.4 ± 2.4 Ma was obtained (Figure 15d; integrated age 55.5 ± 2.5 Ma; isochron age 57.7 ± 3.7 Ma).

DISCUSSION

The large lithological variety of Isla María María Madre rocks provides an excellent local stratigraphic record. This includes regional and contact metamorphism, a Jurassic-Cretaceous-Tertiary magmatic history and sedimentation processes with different detrital sources, witnessing multiple subsidence and uplift events related to the opening of the Gulf of California. Based on field observations and the available geochemical and geochronological data, we developed stratigraphic columns for the southern and central part of the island (Figure 16), summarized as follows:

Folded, banded, and locally migmatitic orthogneisses

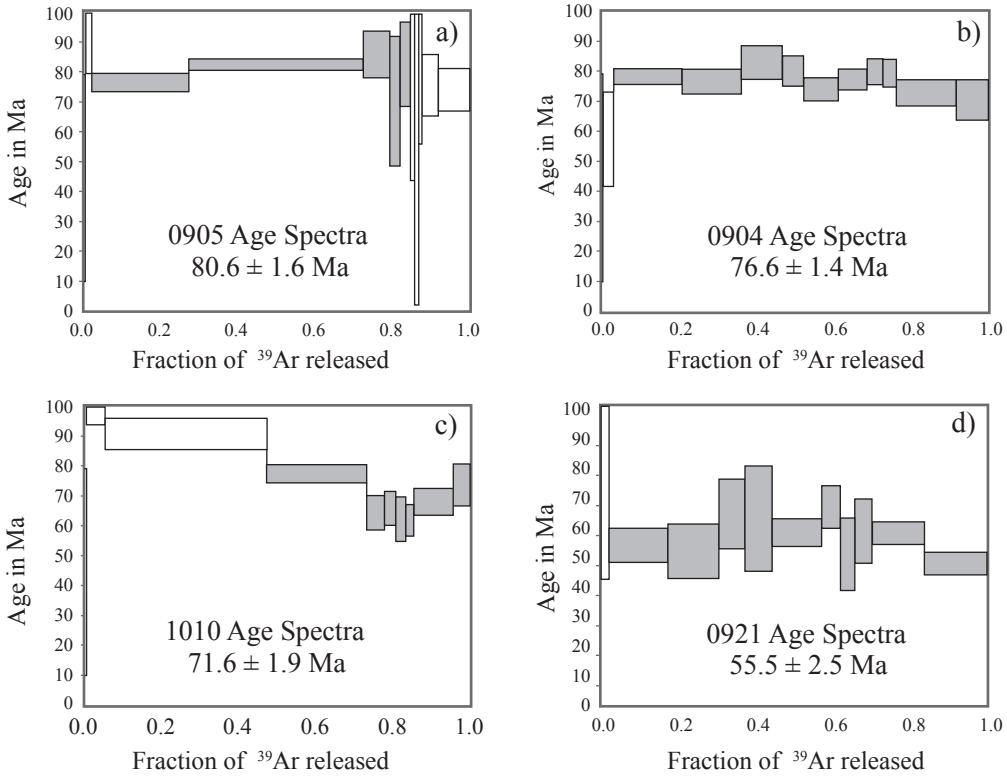

Figure 15. $^{40}Ar/^{39}Ar$ plateau ages for: a) and b) Rhyolitic ignimbrites from the central part of Isla María Madre; c) rhyolitic lava flow from the south-eastern part of the island; and d) deformed and fractured rhyolitic lava flow from the north-western part.

form the oldest exposed basement rocks in the island. These rocks were affected by regional medium- to high-grade metamorphism, locally with anatexis.

Metasedimentary rocks such as calcsilicates and paragneisses are considered as roof pendants of the underlying plutonic rocks. They are affected by contact metamorphism evidenced by abundant skarn in calcsilicates. The age of the sedimentary precursor is unknown, but field observations suggest that it is younger than the gneissic basement.

Plutonic rocks were emplaced during the Late Cretaceous. Pegmatitic dikes represent the ultimate magmatic phase. Mafic dikes with dioritic compositions commonly fill fracture zones within the granitoids, and hence, they are younger than the granitoids.

These three lithological units constitute the "Papelillo Complex", named by its type locality in the Papelillo canyon (Figure 2).

The Papelillo Complex is unconformably overlain by silicic volcanic rocks in the shape of effusive and explosive ignimbrites and lava flows of rhyolithic composition. Effusive rocks can be observed in the highest elevations of the island and are highly tectonized in the southern part. In many locations, these rocks are affected by hydrothermal and deformation processes. According to the obtained $^{40}Ar/^{39}Ar$ ages, these rocks are contemporaneous or younger than the plutonic suite.

The Isla Magdalena sandstone constitutes the oldest sedimentary sequence of Isla María Madre. Although its detrital zircons are considerably younger than those from the overlying Ojo de Buey sequence, its lower stratigraphic position is indicated by field observations (Figure 8c).

Miocene through Pleistocene sedimentary sequences (lower and upper members of the Ojo de Buey sequence) form the most abundant rocks exposed in Isla María Madre. Their foraminiferal and diatomic fossil content characterizes these units as marine to shallow marine sequences, intercalated with some non-marine sandstones (McCloy *et al.*, 1988).

The upper Ojo de Buey sequence contains ash layers, which represent the youngest volcanic event on Isla María María Madre. The hydrothermally altered mafic dikes (sample 0901) and the diabase dikes (sample 1002) SW of Laguna del Toro can also be correlated to this volcanic event.

Both sedimentary sequences (Ojo de Buey sequence and Isla Magdalena sandstone) contain different detrital material. U-Pb zircon ages from the stratigraphically older Isla Magdalena sandstones (Figure 7c) show a dominant peak at 22 Ma (Figure 14f) but no contemporaneous igneous rocks have been identified so far on María Madre and María Magdalena islands. On the other hand, Duque *et al.* (2012) have recently reported similar U-Pb zircon and $^{40}Ar/^{39}Ar$ biotite ages between 18.1 and 25.6 Ma for granitic rocks from Santa Catalina Island, Baja California Sur, from the Pescadero basin of the Gulf of California ocean floor, and

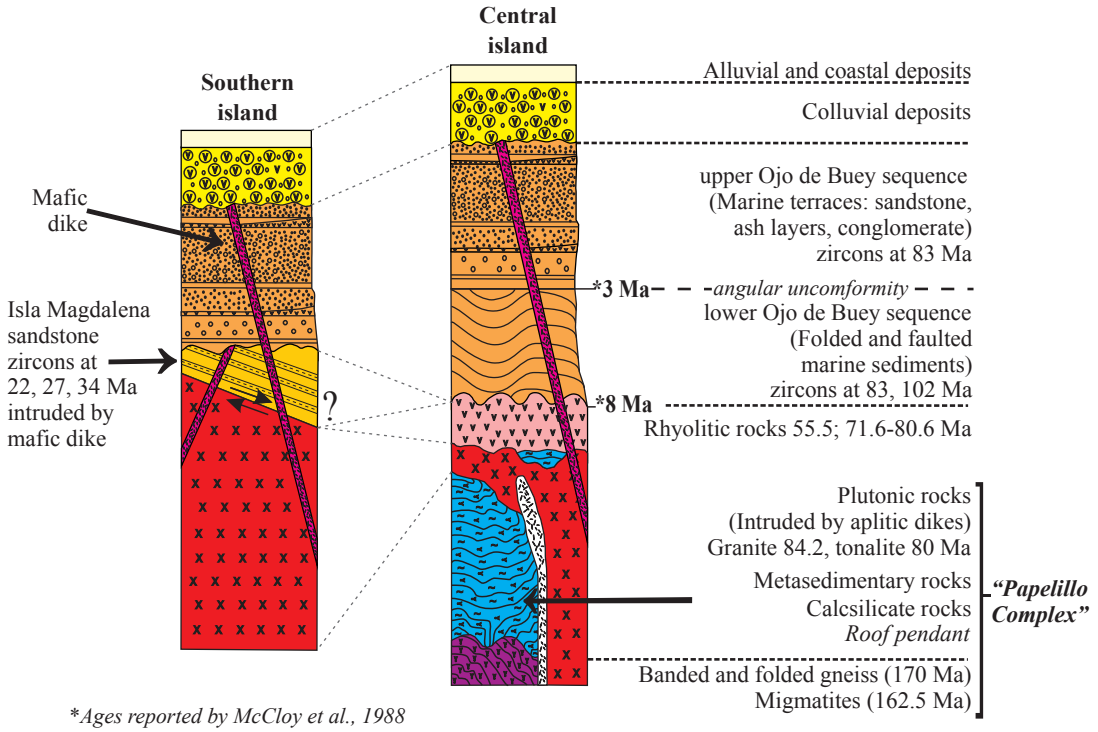

Figure 16. Stratigraphic columns for the southern and north-central Isla María María Madre rock units based on fieldwork and geochronological analyses.

from southern Sinaloa and Nayarit. Such rocks are potential sources for the detritus in the Isla Magdalena sandstone. It is obvious from the zircon data presented here, that these sources did not participate in the sedimentation of the Ojo de Buey sequence. In this Upper Miocene sequence (McCloy *et al.*, 1988), most detrital zircons are of Campanian age (Figuras 14b and d) and probably shed from eroding plutonic and volcanic series of Isla María Madre.

The relative ages among basement rocks are not completely well established, but similar banded, folded, and migmatitic orthogneisses and calcsilicate metasediments were reported from southern Sinaloa (Henry and Fredrikson, 1987) with Jurassic and Jurassic-Lower Cretaceous ages, respectively. Recently Cuéllar-Cárdenas *et al.* (2012) reported a 157 Ma zircon age (U-Pb) from an orthogneiss NE of Mazatlán, Sinaloa. Like those from Isla María Madre, these units were also affected by contact and possibly regional metamorphism and are associated with Cretaceous and Tertiary plutonic rocks. In the Los Cabos Block, Baja California Sur, migmatitic gneisses, deformed granitoids, and calcsilicates have been recognized (Schaaf *et al.*, 2000) and are described in detail by Pérez-Venzor (2012).

On the other hand, the undeformed Isla María Madre plutonic rocks share geochemical and geochronological similarities with their counterparts in Sinaloa (post-tectonic intrusions; Henry and Fredrikson, 1987, Henry *et al.*, 2003), the Los Cabos Block (LCB; Schaaf *et al.*, 2000), and the Puerto Vallarta Batholith (Schaaf *et al.*, 1995). The composition of these granitoids range also from tonalite to granite and their ages are consistent with those from the María Madre granites. In Sinaloa, Henry *et al.* (2003) reported continuous granite emplacement ages between 90 and 45 Ma (U-Pb and K-Ar ages), in the southeastern LCB, Fletcher *et al.* (2007) published U-Pb zircon ages from 75 to 90 Ma, and Pérez-Venzor (2012) obtained intrusion ages of *ca.* 80 Ma (Rb-Sr WR isochrons) for central LCB plutonic rocks. For the Puerto Vallarta Batholith, U-Pb, Rb-Sr, and K-Ar mineral and whole rock ages show a range between 101 and 75 Ma (Schaaf *et al.*, 1995; Fletcher *et al.*, 2007). All intrusions, including those from Isla María Madre, display volcanic-arc environments and are considered as a part of a continuous Cretaceous plutonic belt, extending from northern Baja California (Peninsular Ranges Batholith) to western Mexico, at least to the latitudes of the Jalisco Block. In the light of the new data on Islas Marías igneous rocks, large latitudinal displacements of Baja California Sur as proposed by Beck (1980) or Sedlock *et al.* (1993) can be ruled out.

The Cretaceous and Tertiary ages from María Madre volcanic rocks can be correlated with rhyolitic flows and quartz-latites from the Lower Volcanic Complex (McDowell and Keizer, 1977) of southern Sinaloa, which are described in several publications (Drumble, 1900; Weed, 1902; Hisazumi, 1929; De Cserna and Kent, 1961; Roldan-Quintana and Clark, 1974; Clark, 1976). Henry and Fredrikson (1987) considered them as volcanic equivalents of plutonic rocks. The Lower Volcanic Complex is widely distributed in northwestern Mexico (McDowell and Keizer, 1977) including rocks of the Peninsular Ranges batholiths

of Baja California and its extension into Sinaloa (McDowell and Clabaugh, 1979) with ages from 90 to 40 Ma (*e.g.*, Damon *et al.*, 1983).

The isolated ash layers in the Ojo de Buey sequence and mafic dikes (samples 0901 and 1002) from the southern María Madre coast are still undated, but are considered to represent the youngest volcanic event on the island.

CONCLUSIONS

This work presents for the first time a detailed geological map of María Madre Island, accompanied by an explicit description of the observed geological units and by geochemical and geochronological investigations. Despite its small area of only 145 km^2, a large variety of metamorphic basement rocks, metasediments, granitoids with pegmatitic, aplitic, and mafic dikes, volcanic rocks, and sedimentary covers is exposed.

The metamorphic basement consists of Middle Jurassic orthogneisses and migmatites. Sedimentary sequences were deposited on igneous protoliths and subsequently the entire package was deformed, metamorphosed and affected by an Upper Cretaceous (Campanian) intrusive event. The metasediments are considered as roof pendant of the plutonic suite.

Most sanidine $^{40}Ar/^{39}Ar$ ages indicate that the volcanic sequence is contemporaneous with the plutonic activity and both units display similar major and trace element distributions, suggesting a magmatic consanguinity. Some younger subvolcanic-volcanic events are exposed as dikes and can probably be related to the Neogene Comondú Group (Umhoefer *et al.*, 2001).

The foraminifera and diatom record of Upper Miocene to Pleistocene sediments of the shallow marine Ojo de Buey sequence witness repeated subsidence and uplift events related to the opening of the Gulf of California (McCloy *et al.*, 1988). The detrital zircons in this sequence originate almost exclusively from the Upper Cretaceous igneous María Madre units. The early Miocene? clastic sedimentary rocks exposed along the southern coast of Isla María Madre are correlated according to our field observations to the Isla Magdalena sandstone from the homonymous neighboring island. This sequence is stratigraphically older than the Ojo de Buey sequence but its detrital zircons are considerably younger (around 20 Ma), suggesting different depositional conditions for both units.

The metamorphic and igneous record of Isla María Madre strongly resembles similar Jurassic-Cretaceous plutonic and metamorphic rocks found in the Los Cabos Block of Baja California Sur and volcanic and plutonic rocks from the Mexican continental margin between Sinaloa and Jalisco. Most of these rocks are calc-alkaline and formed in a subduction-related environment.

Taking the above remarks into account, our new data are an important contribution for understanding the evolution of magmatic systems during Cretaceous and Tertiary times in this part of the North American margin. The results obtained so far characterize the María Madre igneous rocks as a part of the Cordilleran batholithic belt that extends from North America to the Isthmus of Tehuantepec and almost certainly exclude large paleotectonic displacements for the Baja California Peninsula.

Further investigations on the other islands of Islas Marías Archipelago are in progress as well as detailed geochemical and isotopic analysis of Isla María Madre rocks to constrain effectively our interpretations.

ACKNOWLEDGEMENTS

This work was supported by DGAPA-PAPIIT grants IN122509 and IN 113012 to P.S. We want to thank Secretaría de Marina, Armada de México, Mazatlán; Secretaría de Seguridad Pública, México (SSP), and Secretaría del Medio Ambiente y Recursos Naturales (SEMARNAT) for the facilities provided to access the study area. Thanks to Rufino Lozano Santa Cruz and Patricia Girón (LUGIS) for XRF analyses, and to Ofelia Pérez (CGEO) for ICP-MS data. Thanks to Jeff Benowitz from the Geochronology Laboratory, University of Alaska at Fairbanks, for $^{40}Ar/^{39}Ar$ analyses; to George Gehrels and Joaquin Ruiz for providing access to the Arizona LaserChron Center that is partially supported by a grant from the Instrumentation and Facilities Program, Division of Earth Sciences, NSF-EAR 0732436, and to Mark Pecha, who was in charge of the LA-MC-ICPMS instrument at Arizona LaserChron Center during our measurements. Reviews by Christopher Henry and Carlos González-León helped to improve the manuscript and are greatly appreciated.

APPENDIX A. SUPPLEMENTARY DATA

Tables A1, A2 and A3 can be found at the journal web site <http://satori.geociencias.unam.mx/>, in the table of contents of this issue.

REFERENCES

Beck, M.E., 1980, Paleomagnetic record of plate-margin tectonic processes along the western edge of North America: Journal of Geophysical Research, 85, 7115-7131.

Brunner, P., 1971, Sobre los ebridons y silico-flagelados de las diatomitas de la Isla María Madre: Revista del Instituto Mexicano del Petróleo, 39(3), 18-25.

Bukry, D., 1978, Pacific Coast Coccolith Stratigraphy between point Conception and Cabo Corrientes, Deep Sea Drilling Project LEG 63, Cabo Corrientes, México (Site 473): United States Geological Survey, Initial Reports, 63, 445-471.

Carreño, A.L., 1985, Biostratigraphy of the Late Miocene to Pliocene on the Pacific Island María Madre: Micropaleontology, 31(2), 139-166.

Carreño A.L., Casey, R.E., Gío-Argáez, R., Martínez-Hernández, E., Pérez-Guzmán, A.M., Reyes-Salas, M., 1979, Estudios

micropaleontológicos en la Isla María Madre, Nayarit: Universidad Nacional Autónoma de México, Revista del Instituto de Geología, 3(2), 193-194.

Clark, K.F., 1976, Geologic section across Sierra Madre Occidental Chihuahua to Topolobambo, México, *in* Woodward, L.A., Northrop, S.A. (eds.), Tectonics and Mineral Resources of Southwestern North America: New Mexico Geological Society Special Publication, 6, 26-38.

Chiñas, L.R., 1963, Bosquejo Geológico de las Islas Marías: México, D.F., Instituto Politécnico Nacional, Escuela Superior de Ingeniería y Arquitectura, B.Sc. Thesis, 62 pp.

Cox, K.G., Bell, J.D., Pankhurst, R.J., 1979, The Interpretation of Igneous Rocks: London, George Allen and Uwin, 450 pp.

Cuéllar-Cárdenas, M.A., Nieto-Samaniego, A.F., Levresse, G., Alaniz-Álvarez, S.A., Solari, L., Ortega-Obregón, C., López-Martínez, M., 2012, Límites temporales de la deformación por acortamiento Laramide en el centro de México: Revista Mexicana de Ciencias Geológicas, 29, 179-203.

Damon, P.E., Shafiqullah, M., Clark, K., 1983, Geochronology of the porphyry copper deposits and related mineralization in Mexico: Canadian Journal of Earth Sciences, 20, 1052-1071.

De Cserna, Z., Kent, B.H., 1961, Mapa geológico de reconocimiento y secciones estructurales de la región de San Blas y El Fuerte, estados de Sinaloa y Sonora: escala 1: 100 000: Universidad Nacional Autónoma de México, Instituto de Geología, Cartas Geológicas y Mineras, núm. 4.

Drumble, E.T., 1900, Notes on the geology of Sonora, México: American Institute of Mining Engineers Transactions, 29, 122-152.

Duque, J., Ferrari, L., Orozco-Esquivel, T., López-Martínez, M., Lonsdale, P., 2012, Rapid exhumation of early to middle Miocene intrusive rocks in the southern Gulf of California: the early stages of continental breakup, *in* Cordilleran Section, 108th Annual Meeting: Geological Society of America, Abstracts with Programs, 44-3, p. 14.

Fletcher, J.M., Grove, M., Kimbrough, D., Lovera, O., Gehrels, G.E., 2007, Ridge-trench interactions and the Neogene tectonic evolution of the Magdalena shelf and southern Gulf of California: Insights from detrital zircon U-Pb ages from the Magdalena fan and adjacent areas: Geological Society of America Bulletin, 119, 1313-1336.

Gehrels, G.E., Valencia, V.A., Ruiz, J., 2008, Enhanced precision, accuracy, efficiency, and spatial resolution of U-Pb ages by laser ablation-multicollector-inductively coupled plasma-mass spectrometry: Geochemistry Geophysics Geosystems, 9(3), 1-13.

Grayson, A.J., 1871, On the physical geography and natural history of the island of the Tres Marías and Socorro off the western coast of México: Proceedings of the Boston Society of Natural History, 14, 261-302.

Hanna, G.D., Grant, W.M., 1926, Expedition to the Revillagigedo Islands, México, in 1925. II. Miocene marine diatoms from María Madre Island, México: Proceedings of the California Academy of Sciences, ser 4, vol.15,115-117.

Henry, C.D., Fredrikson, G., 1987, Geology of part of southern Sinaloa, México adjacent to the Gulf of California: Geological Society of America, Map and Chart Series MCH063, 1-14.

Henry, C.D., McDowell, F.W., Silver, L.T., 2003, Geology and geochronology of granitic batholithic complex, Sinaloa, México: Implications for Cordilleran magmatism and tectonics, *in* Johnson, S.E., Paterson, S.R., Fletcher, J.M., Girty, G.H., Kimbrough, D.L., Martin-Barajas, A. (eds.), Tectonic evolution of northwestern México and the southwestern USA: Geological Society of America, Special Paper 374, 237-274.

Hertlein, L.G., Emerson, W.K., 1959, Pliocene and Pleistocene megafossils from the Tres Marías Islands: American Museum Novitates, 1940, 1-15

Hisazumi, H., 1929, Informe geológico preliminar de la parte norte del Estado de Sinaloa: Anales del Instituto Geológico de México, Tomo 3, p. 95-110

Instituto Nacional de Estadística, Geografía e Informática (INEGI), 1995, Fotografías Aéreas Islas Marías, Vuelo Especial LN:002, escala 1: 75 000: México D.F., Sistema Nacional de Fotografía Aérea (SINFA), Instituto Nacional de Estadística, Geografía e Informática, fotos 17-24.

Instituto Nacional de Estadística, Geografía e Informática (INEGI), 2000, Carta topográfica Isla María Madre F13-C25, escala 1: 50 000: México D.F., Dirección General de Geografía, Instituto Nacional de Estadística, Geografía e Informática, 1 mapa.

Jordan, E.K., Hertlein, L.G., 1926, Expedition to the Revillagigedo Islands, México, in 1925, IV. A Pliocene fauna from María Madre Island, México: Proceedings of the California Academia of Sciences, ser. 4, 15, 209-215.

Lanphere, M.A., Dalrymple, G.B., 2000, First-principles calibration of ^{38}Ar tracers: Implications for the ages of $^{40}Ar/^{39}Ar$ fluence monitors: United States Geological Survey, Professional Paper 1621, 10 p.

Layer, P.W., 2000, Argon-40/Argon-39 age of the El´gygytgyn impact event, Chukotka, Russia: Meteoritics and Planetary Science, 35, 591-599.

Layer, P.W., Hall, C.M., York, D., 1987, The derivation of $^{40}Ar/^{39}Ar$ age spectra of single grains of hornblende and biotite by laser step heating: Geophysical Research Letters, 14, 757-760.

Le Bas, M.J., Le Maitre, R.W., Streckeisen, A., Zanettin, B., 1986, A chemical classification of volcanic rocks based on the total alkali-silica diagram: Journal of Petrology, 27, 745-750.

Lonsdale, P., 1995, Segmentation and disruption of the East Pacific Rise in the mouth of the Gulf of California: Marine Geophysical Research, 17, 323-359.

Lozano-Santa Cruz, R., Bernal, J.P., 2005, Characterization of a new set of eight geochemical reference materials for XRF major and trace elements analysis: Revista Mexicana de Ciencias Geológicas, 22, 329-344.

Ludwig, K.R., 2008, User´s Manual for Isoplot 3.60, A Geochronological Toolkit for Microsoft Excell: Berkeley Geochronology Center, Special Publication No. 4, 77 pp.

Ludwig, K.R., Mundil, R., 2002, Extracting reliable U-Pb ages and errors from complex populations of zircons from Phanerozoic tuffs, *in* 12th Goldschmidt Conference: Geochimica et Cosmochimica Acta, 66, p. 463.

McCloy, C., Ingle, J.C., Barron, J.A., 1988, Neogene stratigraphy, foraminifera diatoms, and depositional history of María Madre Island, México: evidence of Early Neogene marine conditions in the southern Gulf of California: Marine Micropaleontology, 13(3), 193-212.

McDougall, I., Harrison, T.M., 1999, Geochronology and Thermochronology by the $^{40}Ar/^{39}Ar$ method: New York, Oxford University Press, 2nd ed., 269 pp.

McDowell, F.W., Clabaugh, S.E., 1979, Ignimbrites of the Sierra Madre Occidental and their relation to the tectonic history of western Mexico, *in* Chapin, C.E., and Elston, W.E. (eds.) Ash-Flow Tuffs: Geological Society of America, Special Paper 180, 113-124.

McDowell, F.W., Keizer, R.P., 1977, Timing of mid-Tertiary volcanism in the Sierra Madre Occidental between Durango City and Mazatlán, Mexico: Geological Society of America Bulletin, 88,1479-1487.

Mori, L., Gómez-Tuena, A., Cai, Y., Goldstein, S.L., 2007, Effects of prolonged flat subduction on the Miocene magmatic record of the central Trans-Mexican Volcanic Belt: Chemical Geology, 244, 452-473.

Nakamura, N., 1974, Determination of REE, Ba, Fe, Mg, Na, and K in carbonaceous and ordinary chondrites: Geochimica et Cosmochimica Acta, 38, 757-775.

Nelson, E.W., 1899, General description of the Tres Marías Islands, México, *in* Merriam, H.C. (ed.), Natural history of the Tres Marias Islands, Mexico: Washington, United States Department of Agriculture, Division of Biological Survey, North American Fauna, 14, 7-14.

Ness, G.E., 1982, Late Neogene tectonics of the mouth of the Gulf of California: Corvallis, OR, Oregon State University, PhD thesis, 143 pp.

Pearce, J.A., Harris, N.B.W., Tindle, A.G., 1984, Trace element discrimination diagrams for the tectonic interpretation of granitic rocks: Journal of Petrology, 25, 956-983.

Pérez-Guzmán, A.M., 1985, Radiolarian biostratigraphy of the Late Miocene in Baja and the Tres Marías Islands, México: Micropaleontology, 31(4), 320-334.

Pérez-Venzor, J.A., 2012, Estudio geológico-geoquímico del borde oriental del Bloque de los Cabos, Baja California Sur, México: Universidad Nacional Autónoma de México, tesis doctoral, 289 pp.

Ramírez-Rubio, C., 1980, Geología del área de las Islas Marías, *in* V Convención Geológica Nacional, Resúmenes: Sociedad Geológica Mexicana, 23-24.

Roldán-Quintana, J., Clark K.F., 1974, Cenozoic volcanism in relation to mineralization, Sinaloa, México: Geological Society of America, Abstracts with Programs, 6, p. 471.

Ryan, W.B.F., Carbotte, S.M., Coplan, J.O., O´Hara, S., Melkonian, A., Arko, R., Weissel, R.A., Ferrini, V., Goodwillie, A., Nitsche, F., Bonczkowski, J., Zemsky, R., 2009, Global Multi-Resolution Topography synthesis, Geochemistry Geophysics Geosystems, 10 (3), Q03014, doi: 10.1029/2008GC002332.

Samson, S.D., Alexander E.C., 1987, Calibration of the interlaboratory $^{40}Ar/^{39}Ar$ dating standard, MMhb1: Chemical Geology, 66, 27-34.

Schaaf, P., Morán-Zenteno, D., Hernández-Bernal, M., Solís-Pichardo, G., Tolson, G., Köhler, H., 1995, Paleogene continental margin truncation in southwestern México: Geochronological evidence: Tectonics, 14, 1339-1350.

Schaaf, P., Böhnel, H., Pérez-Venzor, J.A., 2000, Pre-Miocene palaeography of the Los Cabos Block, Baja California Sur: Geochronological and palaeomagnetic constrains: Tectonophysics, 318, 53-69.

Sedlock, R.L., Ortega-Gutiérrez, F., Speed, R.C., 1993, Tectonostratigraphic terranes and tectonic evolution of Mexico: Geological Society of America, Special Paper 278, 153 pp.

Stacey, J.S., Kramers, J.D., 1975, Approximation of terrestrial lead isotope evolution by a two-stage model: Earth and Planetary Science Letters, 26, 207-221.

Steiger, R.H., Jäger, E., 1977, Subcomission of geochronology: Convention on the use of decay constants in geo- and cosmochronology: Earth and Planet Science Letters, 36, 359-362.

Sun, S.S., McDonough, W.F., 1989, Chemical and isotopic systematics of oceanic basalts: implications for mantle composition and processes, *in* Saunders A.D., Norr M.J. (eds.) Magmatism in Oceanic Basins: Geological Society of London, Special Publication 42, 313-345.

Umhoefer, P.J., Dorsey, R., Willsey, S., Mayer, L., Renne, P., 2001, Stratigraphy and geochronology of the Comondú Group near Loreto, Baja California Sur, Mexico: Sedimentary Geology, 144, 125-147.

Verma, S.P., 1983, Strontium and neodymium isotope geochemistry of igneous rocks from the North East Pacific and Gulf of California: Isotope Geoscience, 1, 339-356.

Weed, W.H., 1902, Notes on certain mines in the states of Chihuahua, Sinaloa and Sonora, México; American Institute of Mining Engineers Transactions, 32, 396-443.

York, D., Hall, C.M., Yanase, Y., Hanes, J.A., Kenyon, W.J., 1981, $^{40}Ar/^{39}Ar$ dating of terrestrial minerals with a continous laser: Geophysical Research Letters, 8, 1136-1138.

Manuscript received: May 3, 2012
Corrected manuscript received: September 28, 2012
Manuscript accepted: October 3, 2012